World Journal of Stem Cells

Submit a Manuscript: https://www.f6publishing.com

World J Stem Cells 2019 October 26; 11(10): 831-858

DOI: 10.4252/wjsc.v11.i10.831

ISSN 1948-0210 (online)

ORIGINAL ARTICLE

Basic Study

Unmodified autologous stem cells at point of care for chronic myocardial infarction

Alexander Haenel, Mohamad Ghosn, Tahereh Karimi, Jody Vykoukal, Dipan Shah, Miguel Valderrabano, Daryl G Schulz, Albert Raizner, Christoph Schmitz, Eckhard U Alt

ORCID number: Alexander Haenel (0000-0002-5672-0547); Mohamad Ghosn (0000-0001-7670-5363); Tahereh Karimi (0000-0003-4716-1218); Jody Vykoukal (0000-0001-7797-627X); Dipan Shah (0000-0002-6179-2393); Miguel Valderrabano (0000-0002-8401-1684); Daryl G Schulz (0000-0001-7015-9330); Albert Raizner (0000-0001-9857-0519); Christoph Schmitz (0000-0002-4065-1241); Eckhard U Alt (0000-0002-6687-139X).

Author contributions: Raizner A and Alt EU substantially contributed to conception and design of the study; Haenel A, Ghosn M, Karimi T, Vykoukal J, Shah D, Valderrabano M, Schulz DG, Raizner A and Alt EU substantially contributed to acquisition of data; Haenel A, Ghosn M, Karimi T, Vykoukal J, Shah D, Schulz DG, Raizner A, Schmitz C and Alt EU substantially contributed to analysis and interpretation of data; Haenel A, Schmitz C and Alt EU drafted the article; Haenel A, Raizner A, Schmitz C and Alt EU made critical revisions related to important intellectual content of the manuscript; All authors approved the version of the article to be published.

Supported by Alliance of Cardiovascular Researchers (New Orleans, LA 70102, United States), No. 2013-AH-01 (to Haenel A)

Institutional review board statement: This study was

Alexander Haenel, Tahereh Karimi, Eckhard U Alt, Heart and Vascular Institute, Department of Medicine, Tulane University Health Science Center, New Orleans, LA 70112, United States

Alexander Haenel, Daryl G Schulz, Eckhard U Alt, The Methodist Hospital Research Institute, Houston, TX 77030, United States

Alexander Haenel, Department of Radiology and Nuclear Medicine, University Hospital Schleswig-Holstein, Lübeck D-23562, Germany

Mohamad Ghosn, Dipan Shah, Miguel Valderrabano, Albert Raizner, Houston Methodist DeBakey Heart and Vascular Center, Houston, TX 77030, United States

Jody Vykoukal, Department of Translational Molecular Pathology, MD Anderson Cancer Center, The University of Texas, Houston, TX 77030, United States

Christoph Schmitz, Institute of Anatomy, Faculty of Medicine, LMU Munich, Munich D-80336, Germany

Eckhard U Alt, Isar Klinikum Munich, Munich D-80331, Germany

Corresponding author: Eckhard U Alt, MD, PhD, Professor of Medicine, Heart and Vascular Institute, Department of Medicine, Tulane University, Health Science Center, 1340 Tulane Ave., New Orleans, LA 70112, United States. ealt@tulane.edu
Telephone: +1-504-9883040

Abstract

BACKGROUND

Numerous studies investigated cell-based therapies for myocardial infarction (MI). The conflicting results of these studies have established the need for developing innovative approaches for applying cell-based therapy for MI. Experimental studies on animal models demonstrated the potential of fresh, uncultured, unmodified, autologous adipose-derived regenerative cells (UA-ADRCs) for treating acute MI. In contrast, studies on the treatment of chronic MI (CMI; > 4 wk post-MI) with UA-ADRCs have not been published so far. Among several methods for delivering cells to the myocardium, retrograde delivery into a temporarily blocked coronary vein has recently been demonstrated as an effective option.

AIM

To test the hypothesis that in experimentally-induced chronic myocardial

approved by the Institutional Review Board of Houston Methodist Hospital (Houston, TX, United States).

Institutional animal care and use committee statement: The animal use protocol has been reviewed and approved by the Institutional Animal Care and Use Committee at Houston Methodist Hospital (Houston, TX, United States) (AUP-0910-0019).

Conflict-of-interest statement: Schmitz C has served as consultant of SciCoTec (Grünwald, Germany), the principal shareholder of InGeneron, Inc. (Houston, TX, United States). Alt EU is Chairman of the Board of Isar Klinikum and of InGeneron, Inc.

Data sharing statement: Requests for access to data should be addressed to the corresponding author.

ARRIVE guidelines statement: The authors have read the ARRIVE guidelines, and the manuscript was prepared and revised according to the ARRIVE guidelines.

Manuscript source: Unsolicited manuscript

Received: February 18, 2019
Peer-review started: February 20, 2019
First decision: April 15, 2019
Revised: June 5, 2019
Accepted: August 26, 2019
Article in press: August 26, 2019
Published online: October 26, 2019

P-Reviewer: Cao T, Chivu-Economescu M, Grawish ME, Liu L
S-Editor: Ma YJ
L-Editor: Filipodia
E-Editor: Qi LL

infarction (CMI; > 4 wk post-MI) in pigs, retrograde delivery of fresh, uncultured, unmodified, autologous adipose-derived regenerative cells (UA-ADRCs) into a temporarily blocked coronary vein improves cardiac function and structure.

METHODS

The left anterior descending (LAD) coronary artery of pigs was blocked for 180 min at time point T0. Then, either 18 × 10^6 UA-ADRCs prepared at "point of care" or saline as control were retrogradely delivered *via* an over-the-wire balloon catheter placed in the temporarily blocked LAD vein 4 wk after T0 (T1). Effects of cells or saline were assessed by cardiac magnetic resonance (CMR) imaging, late gadolinium enhancement CMR imaging, and post mortem histologic analysis 10 wk after T0 (T2).

RESULTS

Unlike the delivery of saline, delivery of UA-ADRCs demonstrated statistically significant improvements in cardiac function and structure at T2 compared to T1 (all values given as mean ± SE): Increased mean LVEF (UA-ADRCs group: 34.3% ± 2.9% at T1 *vs* 40.4 ± 2.6% at T2, $P = 0.037$; saline group: 37.8% ± 2.6% at T1 *vs* 36.2% ± 2.4% at T2, $P > 0.999$), increased mean cardiac output (UA-ADRCs group: 2.7 ± 0.2 L/min at T1 *vs* 3.8 ± 0.2 L/min at T2, $P = 0.002$; saline group: 3.4 ± 0.3 L/min at T1 *vs* 3.6 ± 0.3 L/min at T2, $P = 0.798$), increased mean mass of the left ventricle (UA-ADRCs group: 55.3 ± 5.0 g at T1 *vs* 71.3 ± 4.5 g at T2, $P < 0.001$; saline group: 63.2 ± 3.4 g at T1 *vs* 68.4 ± 4.0 g at T2, $P = 0.321$) and reduced mean relative amount of scar volume of the left ventricular wall (UA-ADRCs group: 20.9% ± 2.3% at T1 *vs* 16.6% ± 1.2% at T2, $P = 0.042$; saline group: 17.6% ± 1.4% at T1 *vs* 22.7% ± 1.8% at T2, $P = 0.022$).

CONCLUSION

Retrograde cell delivery of UA-ADRCs in a porcine model for the study of CMI significantly improved myocardial function, increased myocardial mass and reduced the formation of scar tissue.

Key words: Adipose tissue-derived regenerative cells; Chronic myocardial infarction; Heart failure; Stem cells; Translational medicine; Point of care cell therapy

Core tip: We report results derived from a feasibility study on pigs whose left anterior descending artery was occluded for 180 min. Four weeks later, 18 × 10^6 fresh, uncultured, unmodified, autologous adipose-derived regenerative cells were retrogradely delivered into the balloon-blocked left anterior descending vein (control: delivery of saline). Another 6 wk later, the mean left ventricular mass (+29%; $P < 0.001$) and cardiac output (+37%; $P = 0.002$) had significantly increased after cell delivery. The unique combination of the procedure used for isolating stem cells and the novel cell delivery route applied in the present study potentially opens new horizons for clinical therapy for chronic myocardial infarction.

Citation: Haenel A, Ghosn M, Karimi T, Vykoukal J, Shah D, Valderrabano M, Schulz DG, Raizner A, Schmitz C, Alt EU. Unmodified autologous stem cells at point of care for chronic myocardial infarction. *World J Stem Cells* 2019; 11(10): 831-858
URL: https://www.wjgnet.com/1948-0210/full/v11/i10/831.htm
DOI: https://dx.doi.org/10.4252/wjsc.v11.i10.831

INTRODUCTION

Heart failure and myocardial infarction (MI) are consequences of ischemic heart disease (IHD)[1]. In recent years cell-based therapies have emerged as a promising strategy to regenerate ischemic myocardium[2-4]. However, the generally disappointing outcome of related clinical trials established a need for developing novel, more effective cell-based therapies for MI[5]. In this regard, it is of note that the treatment of

chronic MI (*i.e.*, patients with a previous MI) (CMI) requires a different approach than the treatment of acute MI (AMI). Specifically, studies on animal models demonstrated that in AMI, cell-based therapies may primarily act *via* anti-apoptotic and anti-inflammatory mechanisms[6], whereas in CMI there is primarily a need for replacing the, often large, loss of contractile tissue[7]. Using a rat model for the study of MI, it was found that apoptosis of both cardiomyocytes and nonmyocytes mostly takes place during the first 4 wk after MI induction[8]. In addition, a study using a rat model for the study of CMI found that the long-term ability of allogeneic mesenchymal stem cells (MSCs) to preserve function in IHD is limited by an immune response, whereby allogeneic MSCs change from an immunoprivileged to an immunogenic state after differentiation[9]. The latter may have substantially contributed to the relatively poor outcome of a recent clinical trial on CMI treatment with allogeneic adipose-derived stem cells (improvement of the left ventricular ejection fraction (LVEF) from an averaged 28.8% to an averaged 31.7% (on average +2.9% absolute change or +10% relative change) at 6-mo follow-up)[10]. Thus, novel approaches for developing cell-based therapies for CMI should be based on the use of autologous MSCs.

Stem cell density has been reported to be significantly higher in adipose tissue than in bone marrow (5% to 10% *vs* 0.1%)[11]. Moreover, fresh, uncultured, unmodified, autologous adipose-derived regenerative cells (UA-ADRCs) [also called stromal vascular fraction (SVF)] have the advantage over culture-expanded adipose-derived stem cells (ASCs) that UA-ADRCs allow for immediate usage at point of care, combined with low safety concerns, since no culturing or modification is applied.

Several experimental studies on animal models have demonstrated the potential of UA-ADRCs for treating AMI[12-14], and a first clinical trial ("APOLLO") showed promising preliminary results[15]. In contrast, no studies on the treatment of CMI (> 4 wk post-MI) with UA-ADRCs have been published.

Thus, it was the aim of the present feasibility study to test in a porcine model for the study of CMI the following hypotheses: (1) Occlusion of the left anterior descending (LAD) coronary artery for three hours results in a clinically-relevant reduction of the LVEF to less than 40% on average 4 wk post-MI (demonstrating significance of the used animal model); (2) Delivery of UA-ADRCs into the LAD vein 4 wk post-MI in this model leads to improved LVEF by more than 15% (relative change) on average 10 wk post-MI (primary objective of this study); and (3) The same animal model shows improvements in cardiac structure 6 wk after delivery of UA-ADRCs (*i.e.*, 10 wk post-MI) (secondary objective of this study).

This study was performed on a porcine model for the study of CMI (experimentally-induced transmural MI) because (1) the pattern of coronary arteries and distribution of blood supply in the porcine heart is remarkably similar to that in the human heart[16]; (2) unlike rodent and rabbit models, porcine models for the study of CMI allow for the application of UA-ADRCs with the same standard of care and the same instrumentation as in humans[12]; and (3) the therapeutic outcome can be evaluated with MRI. The latter is regarded as the technique that allows the most valid (*i.e.*, accurate and reproducible) and comprehensive measurements of cardiac structure (including chamber dimensions, volumes and infarct size in the case of studies on MI) and related cardiac function (including LVEF, cardiac output, stroke volume, end-diastolic volume and end-systolic volume)[17].

MATERIALS AND METHODS

Ethics statement

All experiments were performed in accordance with the guidelines published by the NIH[18], and under a protocol reviewed and approved by the Institutional Animal Care and Use Committee at Houston Methodist Hospital (Houston, TX, United States) (AUP-0910-0019). All appropriate measures were taken to minimize pain and discomfort.

Animal model

Twenty-five pigs (Yorkshire breed; aged 5-7 mo at the index procedures; K Bar Livestock, Sabinal, TX, United States) were randomly assigned by opening sealed envelopes for treatment with UA-ADRCs (n = 13; group 1) or sham-treatment with saline (n = 12; group 2), respectively (a schematic of the overall study design is illustrated in Figure 1). Eight of these animals could not be included in the final analysis for the following reasons: One animal died during anesthesia before MI induction, four animals died during MI induction, one animal had to be euthanized due to a musculoskeletal injury before the end of the study, in one animal the injection of UA-ADRCs deviated from the protocol, and one animal had a pre-existing

cardiac abnormality. As a result, the final analysis was performed on data from nine animals in group 1 and eight animals in group 2.

Induction of myocardial infarction

Myocardial infarction was induced in all animals from groups 1 and 2 at time point T0. Anti-platelet therapy and (after establishing vessel access) anti-coagulant therapy were performed as previously described[13].

Anti-platelet therapy was administered orally, consisting of 325 mg Acetylsalicylic Acid (Aspirin; Bayer, Leverkusen, Germany) 2 d before T0 (*i.e.* on day T0-2), as well as on T0-1, and Clopidogrel (Plavix; Sanofi-Aventis Pharma, Paris, France) with a loading dose of 300 mg on day T0-2 and 75 mg on days T0-1 and T0). In addition, the animals received the beta blocker Bisoprolol (Concor; Merck, Darmstadt, Germany) from T0-2 to T0+5 (1.25 mg per day orally).

Anti-coagulant therapy was intravenously administered after establishing vessel access as follows: Acetylsalicylic Acid 500 mg (Aspisol; Bayer, Leverkusen, Germany), Enoxaparin 1 mg/kg bolus, then 0.5 mg/kg every 4h (Lovenox; Sanofi-Aventis Pharma), and Eptifibatide prior to balloon occlusion in two 180 μg/kg boluses, 10 min apart, followed by a 2 μg/kg/min infusion during balloon occlusion (Integrilin; SP Europe, Bruxelles, Belgium).

A baseline coronary angiography (CA) (Figure 2A) and a ventriculography in the right and left anterior oblique views (RAO/LAO VG) was performed using an Axiom Artis system (Siemens, Erlangen, Germany). Then, a coronary angioplasty balloon (length 9 mm, diameter 3.0-3.5 mm; Maverick OTW; Boston Scientific, Marlborough, MA, United States) was directed over a 0.014" guide wire (Choice Floppy; Boston Scientific) into the LAD artery, and inflated for three hours at the minimal pressure (typically 2 atm) required for a complete occlusion (Figure 2B). After three hours, the balloon was deflated and a post-MI CA was performed to insure vessel patency (Figure 2C). Catheters and sheaths were removed, and the animal was taken care of as previously described[13]. Enoxaparin 1 mg/kg (Lovenox; Sanofi-Aventis Pharma, Paris, France) was subcutaneously administered at the end of the MI induction procedure.

Isolation of adipose-derived regenerative cells

Cells were isolated during catheterization at 4 wk after MI induction (*i.e.*, at time point T1). Following incision with a scalpel, 12-25 g of subcutaneous adipose tissue was harvested from the nuchal region of each pig. The tissue was divided into aliquots of about 6-10 g each. Then, each aliquot was processed using the Transpose RT system (InGeneron, Houston, TX, United States) for isolating UA-ADRCs from adipose tissue. To this end, each aliquot was minced and incubated together with enzymatic Matrase Reagent (InGeneron) for 1 h under agitation in the processing unit at 39°C, according to the manufacturer's instructions for use. Note that UA-ADRCs that were isolated from adipose tissue with the Transpose RT system and the enzymatic Matrase Reagent were comprehensively characterized in a number of studies[19-21]. This included the demonstrated expression of the regenerative cell-associated genes Oct4, Klf4 and Hes3[21], as well as their differentiative potential into adipogenic, osteogenic, hepatogenic and neurogenic cell lines[21]. On this basis, UA-ADRCs isolated from adipose tissue with the Transpose RT system and the enzymatic Matrase Reagent were used in a number of clinical pilot trials[22-24], and are currently under investigation in a number of Investigational Device Exemption (IDE) studies approved by the United States Food and Drug Administration[25-29].

Characterization of adipose-derived regenerative cells

UA-ADRCs were characterized by cell counting, measuring cell viability, colony-forming unit (CFU-F) assays and flow cytometry.

For counting cells, they were stained with fluorescent nucleic acid stain (SYTO13; Life Technologies, Grand Island, NY, United States) following the manufacturer's instructions, and then counted using a hemocytometer under an Eclipse Ti-E inverted fluorescence microscope (Nikon Corporation, Tokyo, Japan) using a PlanFluor 10 × objective [numerical aperture (NA) = 0.3] (Nikon).

The viability of UA-ADRCs was determined by preparing a 3:1 dilution of the cell suspension in 0.4% Trypan Blue solution. Nonviable cells were counted using a hemocytometer under the same microscope, and were correlated to the number of viable nucleated cells.

The CFU-F assay was implemented as an indicator of stemness[30]. To this end, freshly isolated nucleated cells from each preparation of UA-ADRCs were plated at a density of 100,000 cells per 35-mm-diameter well in triplicate, and incubated for 14 d in standard growth media as previously described[31]. Media were changed twice weekly. Afterwards, the cells were fixed with 4% formalin, stained with hematoxylin for 10 min and washed with phosphate-buffered saline (PBS). Photomicrographs were

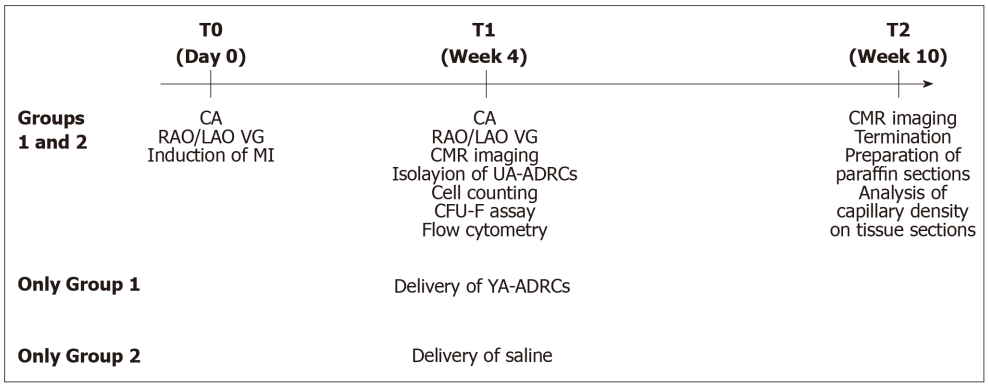

Figure 1 Experimental details of the present study. CA: Coronary angiography; RAO/LAO VG: Ventriculography in right and left anterior oblique views; MI: Myocardial infarction; CMR: Cardiac magnetic resonance; UA-ADRCs: Fresh, uncultured, unmodified, autologous adipose-derived regenerative cells.

taken from five randomly chosen fields-of-view per well with a DS-Fi1 CCD color camera (2560 x 1920 pixels) (Nikon) attached to an Eclipse Ti-E inverted microscope (Nikon) and NIS-Elements AR software (version 4.13) (Nikon), using a Plan EPI 2.5× objective (NA = 0.075) (Nikon). A colony-forming unit was defined as a cluster containing at least ten fibroblast-like fusiform cells[20]. Two experienced investigators individually counted the colonies.

For flow cytometric analysis, UA-ADRCs were cultured for 24 h, incubated with antibodies for 30 min, washed, re-suspended in 1 mL PBS with 10% fetal bovine serum and 1% sodium azide, and directly analyzed by flow cytometry employing a BD FACSAria Fusion device (BD Bioscience, San Jose, CA, United States). Antibodies against porcine CD29 (antibodies-online, Aachen, Germany), CD44 (Abcam, Cambridge, MA, United States), NG2 (Abcam), Oct4 (Novus Biologicals, Littleton, CO, United States), CD31 (Gentex, Irvine, CA, United States), CD45 (Abcam), Nestin (Santa Cruz Biotechnology, Dallas, TX, United States), CD146 (Gentex, Irvine, CA, United States) and CD117 (eBioscience, San Diego, CA, United States) were used.

Delivery of cells or saline as controls

Four weeks after MI induction, a 6F Amplatz right 1 guide catheter (Mach 1; Boston Scientific) was advanced over a 0.035'' wire (J-tip Starter; Boston Scientific) through the jugular vein into the coronary sinus (CS). Once in place in the CS, an angioplasty balloon (length 8-12 mm; diameter 3.0-3.5 mm; Maverick OTW; Boston Scientific) was positioned over a 0.014'' guide wire (Choice Floppy; Boston Scientific) at the site of the LAD vein that corresponded to the previous LAD artery occlusion site (Figure 2D). After the wire was removed, either a suspension of UA-ADRCs (18×10^6 cells in 10 mL saline; group 1) or 10 mL saline alone (group 2), respectively, were delivered at a rate of approximately 0.25 mL/s through the catheter's central lumen retrogradely into the LAD vein. The angioplasty balloon was kept inflated during the entire delivery procedure, and for five minutes after the delivery. Operators were blinded to the group assignment, *i.e.*, they did not know whether UA-ADRCs or saline was delivered.

Cardiac magnetic resonance (CMR) imaging

All animals underwent CMR)imaging directly before the delivery of UA-ADRCs or saline at T1, as well as 6 wk after T1 (*i.e.* at T2). The scans were performed using a 1.5 Tesla MRI scanner (Avanto; Siemens).

Steady-state free precession (SSFP) CMR cine images were acquired using an electrocardiogram-gated SSFP pulse sequence in multiple short-axis and long-axis views. Short-axis views were obtained every 1 cm from the atrioventricular ring to the apex to cover the entire left ventricle (slice thickness 6 mm, inter-slice gap 4 mm, echo time (TE) 1-1.5 ms, temporal resolution (TR) 35–45 ms, flip angle 50-90°).

Late gadolinium enhancement (LGE) CMR imaging was performed approximately ten minutes after the administration of 0.15 to 0.20 mmol/kg of gadolinium (Magnevist; Bayer Inc. Mississauga, ON, Canada) in slice orientations identical to CMR cine imaging using a standard inversion recovery gradient echo pulse sequence. Manual adjustment of the time from inversion (TI) was performed in all cases in order to achieve the nulling of normal viable myocardium[32]. Typical imaging parameters were matrix 256 × 192, slice thickness 6 mm, gap 4 mm, TI 250–350 ms, TE 2.0–2.5 ms, flip angle 30°, and parallel imaging with a two-fold acceleration factor.

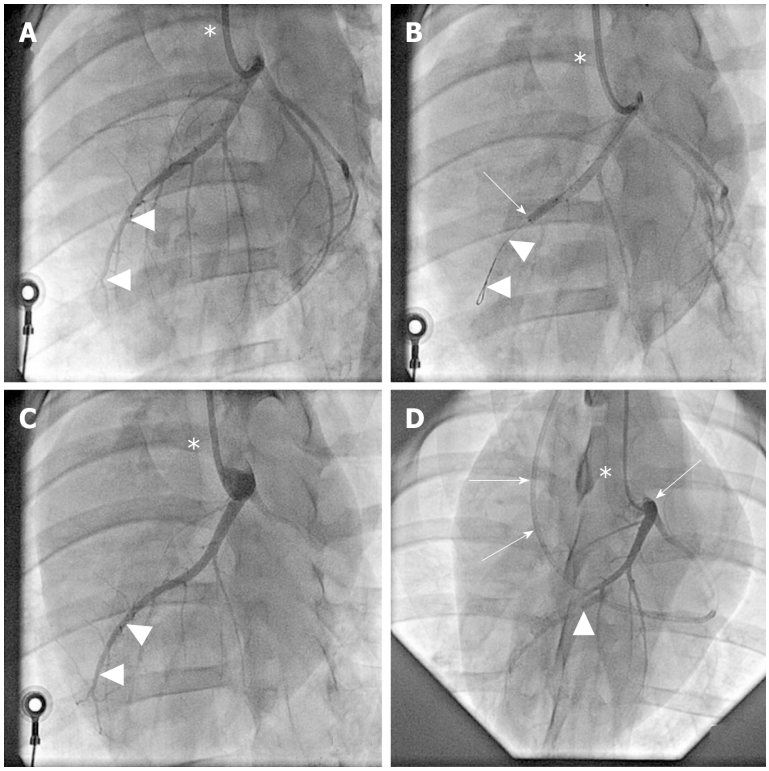

Figure 2 Angiographic details of the present study. A: Baseline coronary angiography of a porcine heart in a left anterior oblique view (in all panels, the white asterisk indicates the angiography catheter positioned in the left main coronary ostium). The white arrowheads indicate the distal LAD artery; B: Induction of myocardial infarction by occlusion of the LAD artery for three hours through an inflated balloon catheter at time point T0. The white arrow indicates the position of the inflated balloon inside the mid LAD artery, whereas the white arrowheads show the guidewire in the distally occluded LAD artery; C: Complete reperfusion of the LAD artery (white arrowheads) three hours after removal of the balloon occlusion; D: Delivery of fresh, uncultured, unmodified, autologous adipose-derived regenerative cells (or saline as control, respectively) through the LAD vein (matching the initial LAD artery occlusion site) into the infarction area 4 wk later (*i.e.* at time point T1). To this end, the LAD vein was occluded with an inflated "over the wire" balloon catheter advanced through a guiding catheter (black arrows), placed from the right jugular vein into the right atrium and then into the coronary sinus. The inflated balloon (filled with contrast dye; white arrowhead) in the coronary LAD vein had the aim to prevent the backflow of cells when they were delivered through the distal orifice of the central lumen of this balloon catheter. LAD: Left anterior descending.

Analysis of CMR images

Image analysis was performed with cvi[42] software (Circle Cardiovascular Imaging Inc., Calgary, AB, Canada). Endocardial and epicardial borders were traced using planimetry on stacks of short-axis cine images in end diastole and end systole (Figure 3). Based on these data, the following variables were calculated for each animal: LVEF, cardiac output, stroke volume, end-diastolic volume (EDV), end-systolic volume (ESV) and left ventricular mass. LVEF was calculated as the difference between EDV and ESV, divided by EDV. The left ventricular mass was calculated by the difference between the left ventricular epicardial and endocardial volumes during end systole, multiplied by myocardial density (1.05 g/cm^3)[33]. For quantification of scar tissue, a region of normal myocardium was independently chosen on each short axis image showing the left ventricle, and hyper-enhanced regions in each slice were located. Hyper-enhancement was identified as areas of signal intensity ≥ 5 standard deviations greater than normal myocardium[34]. Two well-trained MRI physicians, blinded to the group assignment, evaluated the selected regions and graded the findings in all segments on each short axis image.

Analysis of regional replacement fibrosis

This analysis was performed with the cvi[42]® software (Circle Cardiovascular Imaging Inc.) on the LGE CMR images as follows: (1) The left ventricle was divided into 17 segments, as recommended by the American Heart Association (AHA)[35]. With the exception of the apical segment (No. 17), which cannot be investigated on the short axis, transversal images through all segments of the mid left ventricle of a porcine heart that were applied in this study (Figure 3) were analyzed, yielding a total of 9×16 (group 1) + 8×16 (group 2) = 272 analyzed segments; (2) The signal intensity (SI) of a

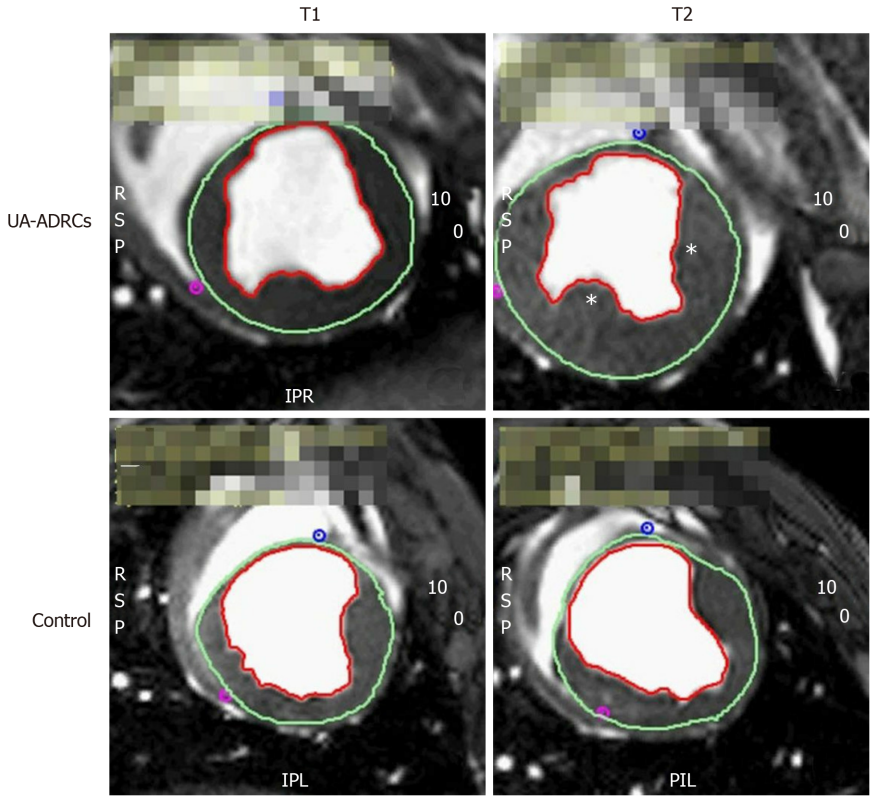

Figure 3 Steady-state free precession CMR imaging of the porcine heart. A-D: Representative examples of end-systolic, short axis, transversal images through the mid left ventricle of a porcine heart obtained with SSFP CMR imaging for analyzing hemodynamic parameters and wall motility at time points T1 (A, C) and T2 (B, D) of a representative animal in group 1 (delivery of UA-ADRCs) (A, B) and a representative animal in group 2 (control) (C, D) (details are provided in the main text). In all panels, the epicardial contours are highlighted in green, and the endocardial contours in red. Note the increased end-systolic thickness of the left ventricular wall at T2 after delivery of UA-ADRCs at T1 (asterisks in B) compared to the delivery of saline at T1 (D). In the examples presented here, the left ventricular ejection fraction was 27.2% in (A), 39.7% in (B), 22.5% in (C), and 27.2% in (D). CMR: Cardiac magnetic resonance; SSFP CMR: Steady-state free precession cardiac magnetic resonance; UA-ADRCs: Fresh, uncultured, unmodified, autologous adipose-derived regenerative cells.

given pixel was considered hyper-enhanced when its SI was ≥ 5 standard deviations greater than the SI of normal myocardium (SI > 5 SD); otherwise, its SI was considered normal[34]; (3) For each segment, the relative number of pixels with hyper-enhanced SI was calculated ($NPrel_{SI>5SD}$). These calculations were separately performed for T1 and T2, resulting in segment-specific data $NPrel_{SI>5SD}$-T1 and $NPrel_{SI>5SD}$-T2; and (4) For all segments of a given animal, the difference between $NPrel_{SI>5SD}$-T1 and $NPrel_{SI>5SD}$-T2 was calculated as $\Delta NPrel_{SI>5SD}$ = $NPrel_{SI>5SD}$-T2 - $NPrel_{SI>5SD}$-T1.

Termination

Animals were euthanized according to the Houston Methodist Research Institute Euthanasia for Large Animals Procedure (Houston, TX, United States) after performing CA, RAO/LAO VG and CMR imaging at T2. Intravenous injection of 0.25 mg/kg Pentobarbital/Phenytoin combination was performed in conjunction with isoflurane overdose. Death was verified by the absence of vital signs. Hearts and organs were removed for further histologic and immunofluorescence analysis. Animal carcasses were disposed of in accordance with standard operating procedures of the Houston Methodist Research Institute (Houston, TX, United States).

Histologic processing of heart tissue

Hearts were harvested and fixed in 5% paraformaldehyde. The left ventricle was cut into six transversal, 1 cm-thick slices from apex to base. Then, from each heart, several approximately 1 cm × 1 cm × 1 cm large tissue samples were collected, representing the left ventricular border zone of MI, the core region of MI, and regions of viable myocardium. Specimens were paraffin-embedded and cut into 5 μm-thick tissue sections that were mounted on glass slides and stained with Masson's Trichrome staining, or processed with fluorescence immunohistochemistry.

Fluorescence immunohistochemistry was performed on de-paraffinized and rehydrated sections that were washed with PBS containing 0.3% Triton X-100 (Sigma Aldrich, St. Louis, MO, United States) and blocked with 10% casein solution (Vector Laboratories, Burlingame, CA, United States) for 30 min at room temperature. Then, sections were incubated overnight with diluted Rabbit anti-von Willebrand factor (vWF) primary antibody (Abcam) or diluted Rabbit anti-adiponectin (Cy5 conjugated) primary antibody (Biorbyt, San Francisco, CA, United States), and subsequently for 1 h with diluted Goat anti rabbit-IgG secondary antibody (Cy5 conjugated) (Thermo Scientific, Waltham, MA, United States). Counterstaining of nuclei and mounting were performed with Vectashield Antifade Mounting Medium with DAPI (Vector Laboratories).

Analysis of microvessel density

The microvessel density was determined on up to four representative sections from each animal showing the left ventricular border zone of MI. Only sections that showed at least 30% of both scar tissue and viable myocardium were considered in this analysis. To this end, photomicrographs covering the entire section were taken with a DS-Fi1 CCD color camera (Nikon) attached to an Eclipse Ti-E inverted microscope (Nikon) using a PlanApo 20× objective (NA = 0.75) (Nikon). Images were analyzed using ImageJ software (U. S. National Institutes of Health, Bethesda, MD, United States). Using a defined grid of ten fields per section with an area of 0.3 mm^2 per field, two independent, blinded evaluators determined the number of microvessels per field (microvessels with a diameter between 2 and 10 μm were counted). Microvessel density was calculated based on microvessel counts on a total of 202 fields (animals in group 1) or 247 fields (animals in group 2), respectively.

Photography

The photomicrographs shown in Figures 4-6 were produced by digital photography using a DS-Fi1 CCD color camera (2560 x 1920 pixels; Nikon) (Figures 4 and 5) or a CoolSNAP HQ2 CCD monochrome camera (1392 x 1040 pixels; Photometrics, Tucson, AZ, United States) (Figure 6) attached to an Eclipse Ti-E inverted microscope (Nikon) and NIS-Elements AR software (Nikon), using the following objectives (all from Nikon): PlanFluor 4 × (NA = 0.13), 10× (NA = 0.3) and 20× (NA = 0.45). The final figures were constructed using Corel Photo-Paint X7 and Corel Draw X7 (both versions 17.5.0.907; Corel, Ottawa, Canada). Only minor adjustments of contrast and brightness were made using Corel Photo-Paint, without altering the appearance of the original materials.

Statistical analysis

For each combination of animal groups [group 1 (delivery of UA-ADRCS) and group 2 (control)], time point [T1 (4 wk after MI induction) and T2 (10 wk after MI induction)], the mean ± SE were calculated for the following variables: LVEF, cardiac output, stroke volume, EDV, ESV, heart rate, left ventricular mass and relative amount of scar tissue. Group-specific means and SEM were also calculated for the body weight of the animals (determined at T0, T1 and T2) and the microvessel density (investigated only at T2). These calculations were performed with previous testing with the Shapiro-Wilk normality test of whether the values came from a Gaussian distribution. Except for the microvessel density, comparisons between groups were performed with repeated measures two-way analysis of variance, followed by post hoc Bonferroni tests for pairwise comparisons. For microvessel density, comparisons between groups were performed with the unpaired two-tailed Student's *t*-test.

Mean and SEM were also calculated for the variable $\Delta NPrel_{SI>5SD}$ (results of the regional replacement fibrosis analysis). This was separately undertaken for each combination of animal groups (groups 1 and 2) and segments (those that are assigned to the territory of the LAD artery in the human heart, and those that are assigned to the territory of the right coronary artery and the left circumflex coronary artery in the human heart). Comparisons between groups were performed with two-way analysis of variance, followed by post hoc Bonferroni tests for pairwise comparisons.

In all analyses, an effect was considered statistically significant if its associated p value was smaller than 0.05. Calculations were performed using GraphPad Prism (version 7.0 for Windows, GraphPad software, San Diego, CA, United States).

RESULTS

Characterization of UA-ADRCs

The amount of adipose tissue that was obtained from the nuchal region per pig varied between 12-25 g (mean ± SE: 18.1 ± 1.61 g). On average, $0.98 \times 10^6 \pm 0.10 \times 10^6$

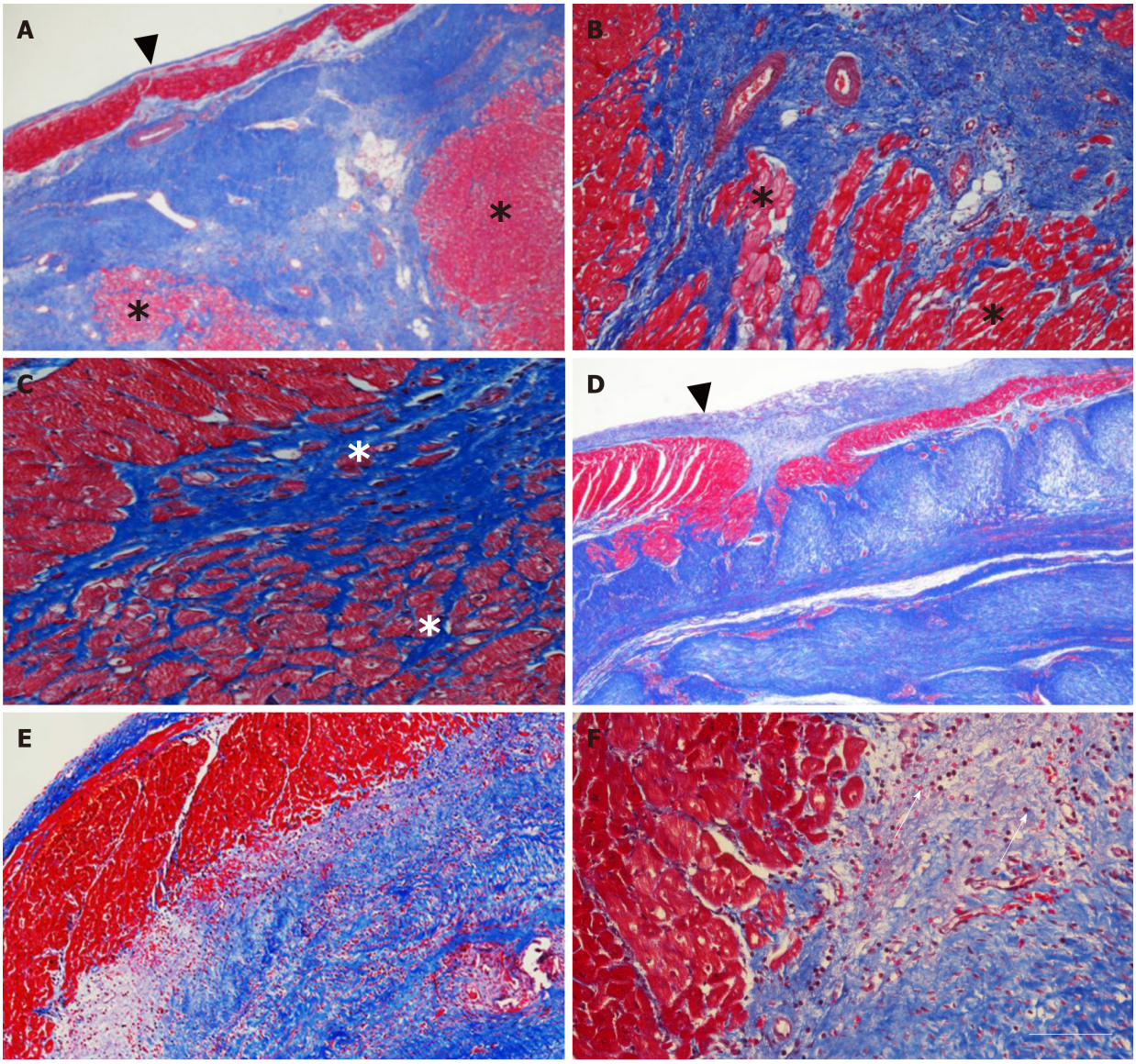

Figure 4 Microstructure of cardiac tissue after delivery of UA-ADRCs or saline. A-F: Representative photomicrographs of paraffin-embedded, 5 μm thick tissue sections stained with Masson's Trichrome staining of post mortem hearts from pigs in group 1 (delivery of fresh, uncultured, unmodified, autologous adipose-derived regenerative cells) (A-C) and group 2 (delivery of saline as control) (D-F) at T2. The arrowheads in (A, D) point to the endocardium, the asterisks in (A-C) indicate patchy islets of cardiomyocytes located within areas of fibrous tissue, and the arrows in (F) point to an infiltration with inflammatory cells. The scale bar in (F) represents 500 μm in (A, D), 200 μm in (B, E), and 100 μm in (C, F). UA-ADRCs: Fresh, uncultured, unmodified, autologous adipose-derived regenerative cells.

nucleated cells were isolated from each gram of adipose tissue (cell yield), from which 93.3% ± 0.4% cells were viable (live cell yield). The CFU-F value was 11.3%. Flow cytometric analysis demonstrated the following relative numbers of cells immunopositive for a certain marker (sorted in descending order; an example of the results of flow cytometric analysis is depicted in Figure 7): CD29: Between 44.1-52.9% (mean: 48.5%); CD44: Between 34.2-39.8% (mean: 37.0%); CD31: Between 6.0-16.7% (mean: 11.4%); NG2: Between 7.3-12.3% (mean: 9.8%); CD45: Between 3.9-13.9% (mean: 8.9%); Oct4: Between 2.4-6.2% (mean: 4.3%); Nestin: Between 1.9-6.2% (mean: 4.1%); CD146: Between 0.4-0.7% (mean: 0.6%); and CD117: Between 0.1-0.4% (mean: 0.3%).

Improvement of cardiac function after delivery of UA-ADRCs

The following, statistically significant improvements in cardiac function at T2 compared to T1 were found for the animals in group 1 (delivery of UA-ADRCs) but not for the animals in group 2 (control): Increased mean left ventricular ejection fraction (+18%; $P = 0.037$) (primary objective) (Figure 8A and B; mean and SEM data as well as P-values of repeated measures two-way analysis of variance are provided in Table 1), increased mean cardiac output (+37%; $P = 0.002$) (Figure 8C and D, as well as Table 1), and increased mean stroke volume (+41%; $P < 0.001$) (Figure 8E and 8F, as

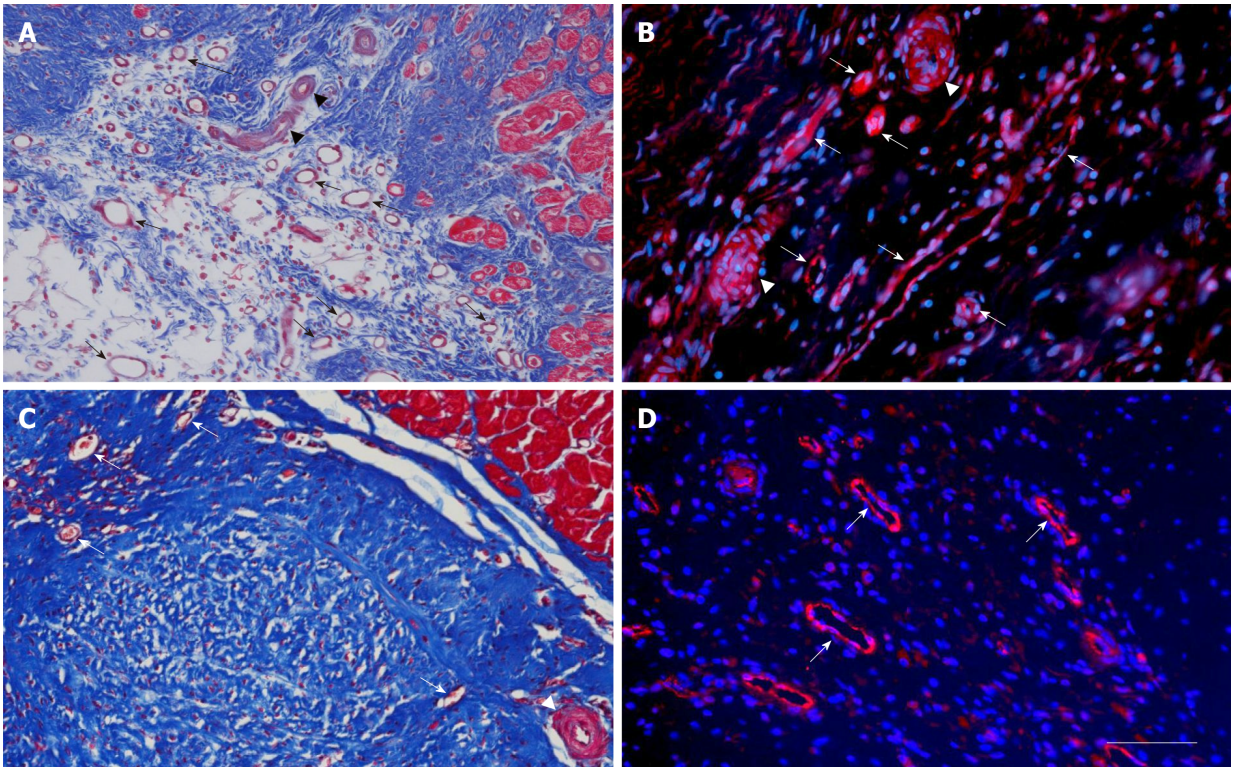

Figure 5 Microvessel density after delivery of UA-ADRCs or saline. The panels show representative photomicrographs of paraffin-embedded, 5 μm thick tissue sections of post mortem hearts from pigs in group 1 (delivery of fresh, uncultured, unmodified, autologous adipose-derived regenerative cells) (A, B) and group 2 (delivery of saline as control) (C, D) at T2. In (A, C), tissue sections were stained with Masson's Trichrome staining. In (B, D), tissue sections were processed with fluorescence immunohistochemistry in order to detect von Willebrand factor (red) (counterstaining with DAPI in blue). The arrows point to microvessels, and the arrowheads to small arterioles. The scale bar shown in D represents 100 μm in (A, C) and 35 μm in (B, D). UA-ADRCs: Fresh, uncultured, unmodified, autologous adipose-derived regenerative cells.

well as Table 1).

As animals in both groups grew from T1 to T2 (Figure 9), the mean end-diastolic volume significantly increased in both groups from T1 to T2 [group 1: +20% (P < 0.001); group 2: +15% (P = 0.004)] (Figure 8G and H, as well as Table 1). However, the mean end-systolic volume significantly increased only in group 2 (+17%; P = 0.018) but not in group 1 (+9%; P = 0.222) (Figure 8I and J, as well as Table 1), causing a significant increase in mean stroke volume in group 1 (+41%; P < 0.001) but not in group 2 (+10%; P = 0.552). The mean heart rate showed no significant difference between T1 and T2 in both groups (Figure 8K and L, as well as Table 1), causing a significant increase in mean cardiac output only in group 1 (+37%; P = 0.002) but not in group 2 (+7%; P = 0.798).

Improvement of cardiac structure after delivery of UA-ADRCs

For animals in group 1 (delivery of UA-ADRCs) but not in group 2 (control), a significantly increased mean mass of the left ventricle (+29%; P < 0.001) was found at T2 compared to T1 (Figure 10A and C; results of statistical analysis are summarized in Table 1). Furthermore, animals in group 1 (delivery of UA-ADRCs) showed a significantly decreased mean relative amount of scar volume of the left ventricular wall (-21%; P = 0.042) at T2 compared to T1 (Figure 10B and D, Figure 11 and Table 1). Of note, the opposite was observed for animals in group 2 (control), *i.e.*, a significant increase in the mean relative amount of scar volume of the left ventricular wall (+29%; P = 0.022) at T2 compared to T1 (Figure 10B and D, Figure 11 and Table 1).

The regional replacement fibrosis data were visualized using color-coded, AHA 17-segment bullseye plots (Figure 12). Statistical analysis demonstrated significant improvement in LAD segments – but not in non-LAD segments – after delivery of UA-ADRCs (P = 0.008) (results of repeated measures two-way analysis of variance: $P_{Interaction}$ = 0.125; $P_{Territory}$ = 0.936; $P_{Treatment}$ < 0.001) (Figure 13).

Histologic examination demonstrated patchy islets of cardiomyocytes located within areas of fibrous tissue in the left ventricular border zone of the MI in post-mortem hearts of animals in group 1 (delivery of UA-ADRCs) (Figure 4A, 4B and 4C). In contrast, the post mortem hearts of animals in group 2 (control) showed infiltration with inflammatory cells in the same region (Figure 4D, 4E and 4F).

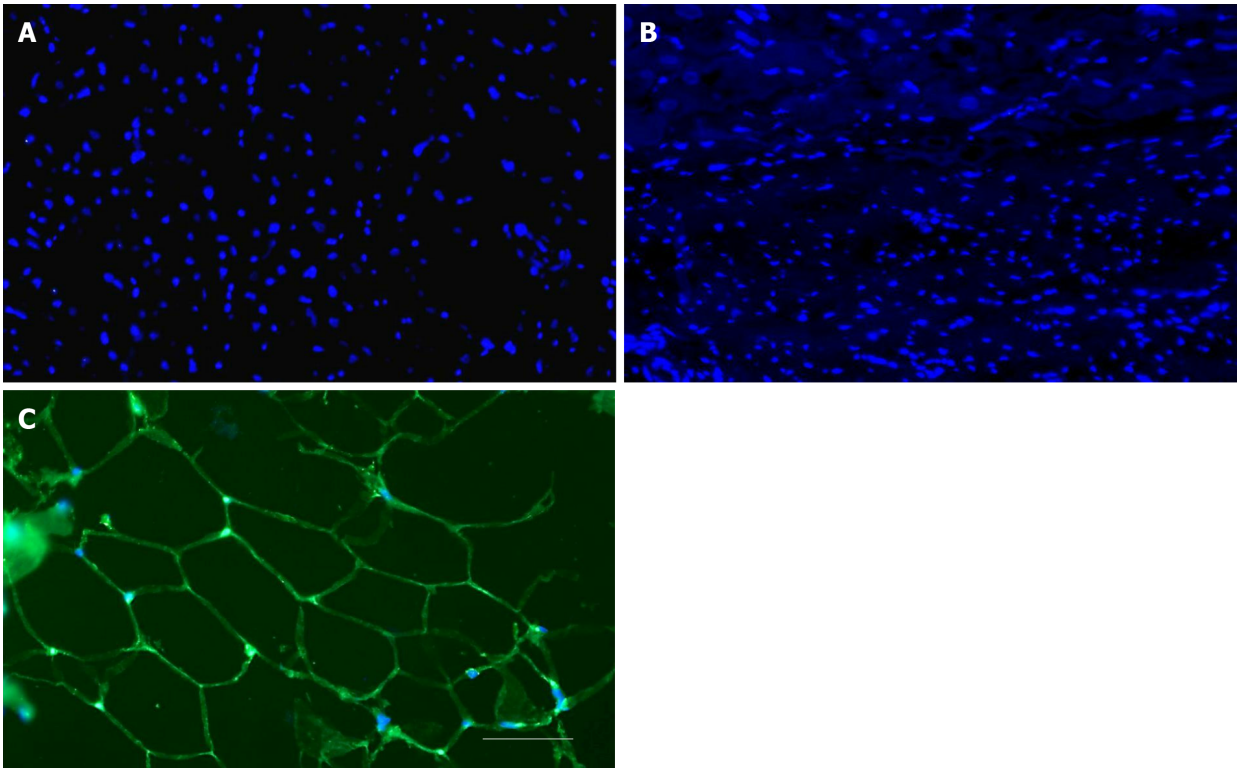

Figure 6 No differentiation of stem cells into adipocytes after delivery of UA-ADRCs. A, B: Representative photomicrographs of paraffin-embedded, 5 μm thick tissue sections of post mortem hearts from pigs in group 1 (delivery of fresh, uncultured, unmodified, autologous adipose-derived regenerative cells) (A) and group 2 (delivery of saline as control) (B), taken from the left ventricular border zone of myocardial infarction at 10 wk. (C) Representative photomicrograph of a paraffin-embedded, 5 μm thick tissue section of subcutaneous adipose tissue from a pig. The sections were stained with DAPI (blue), and processed for immunofluorescent detection of adiponectin (green). The scale bar represents 100 μm. UA-ADRCs: Fresh, uncultured, unmodified, autologous adipose-derived regenerative cells.

Improvement of cardiac revascularization after delivery of UA-ADRCs

The left ventricular border zone of the MI of the post-mortem hearts in group 1 animals (delivery of UA-ADRCs) exhibited a significant, more than two-fold higher mean microvessel density than the corresponding region in the post-mortem hearts of the group 2 animals (control) at T2 [54.4 ± 3.7 *vs* 26.1 ± 2.8 (mean ± SE) capillaries per mm^2; $P < 0.001$] (Figure 5A and C). Immunofluorescent detection of von Willebrand factor supported this finding (Figure 5B and D).

No differentiation of stem cells into adipocytes after delivery of UA-ADRCs

Cells in the left ventricular border zone of the MI of the post-mortem hearts from the group 1 (delivery of UA-ADRCs) and 2 (control) animals displayed no expression of adiponectin at T2 (Figure 6).

DISCUSSION

This is the first study in which all of the following findings from previous research on cell-based therapies for CMI with high clinical relevance were considered and combined into a single model: (1) Application of the same standard of care and instrumentation as in humans by using a porcine model for the study of CMI (which is not possible when investigating mouse or rat models for the study of CMI); (2) A low baseline LVEF after induction of MI of approximately 35% (according to the guidelines for the diagnosis and treatment of acute and chronic heart failure published by the European Society of Cardiology in 2016[36] (a LVEF ≥ 50% is considered normal or preserved, whereas a LVEF < 40% is considered reduced) (the mean LVEF of healthy landrace pigs with an average body weight of approximately 53 kg is approximately 53%[37]); (3) The use of well-characterized, fresh, uncultured, unmodified autologous adipose-derived regenerative cells prepared at "point of care" (rather than employing cultured and/or modified, autologous or non-autologous cells); and (4) The evaluation of therapeutic success using CMR imaging (rather than using other methods such as echocardiography). Besides this, the UA-ADRCs were retrogradely delivered into the temporarily blocked LAD vein (rather than

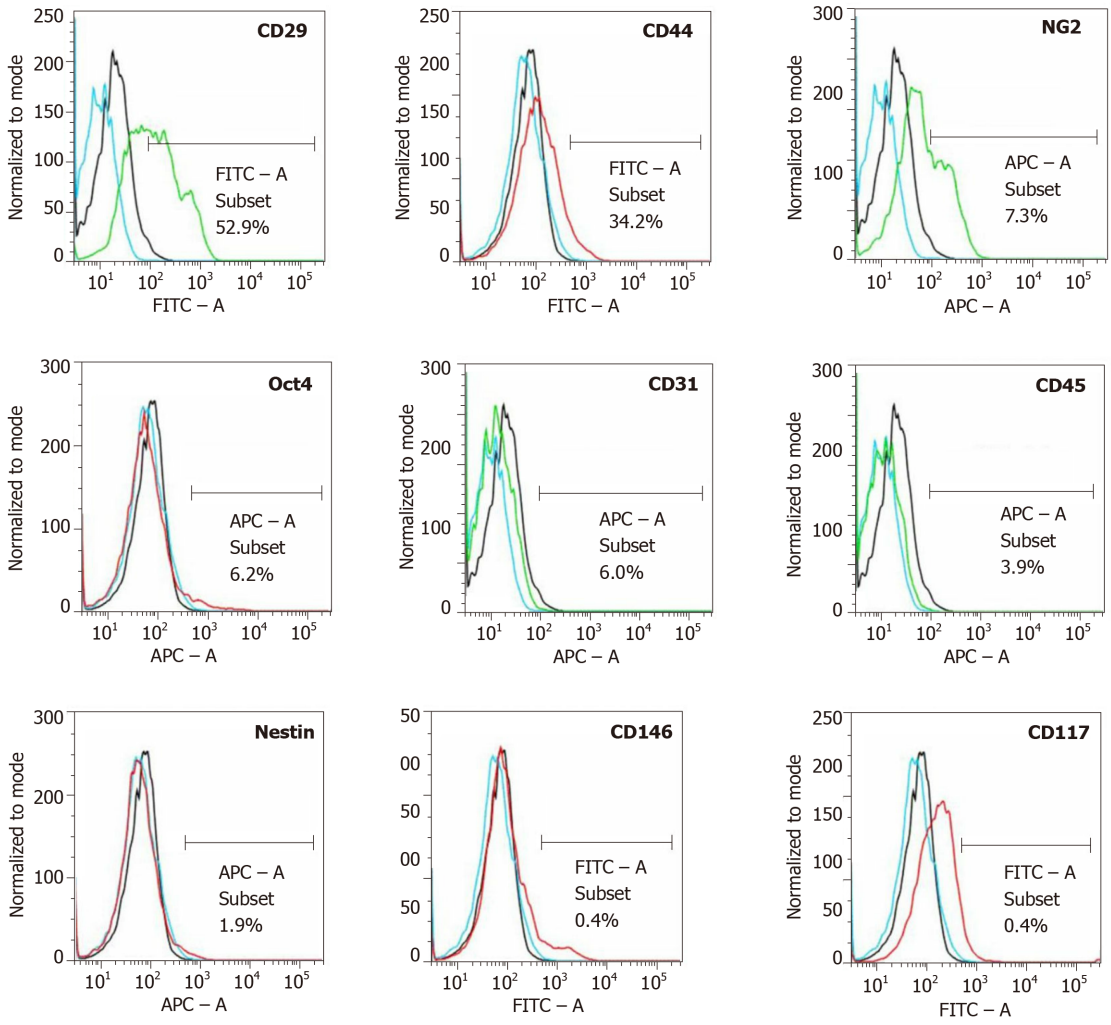

Figure 7 Analysis of cell surface markers of fresh, uncultured, unmodified, autologous adipose-derived regenerative cells from an animal in group 1 using flow cytometry. The cells were stained with monoclonal antibodies for CD29, CD44, NG2, Oct4, CD31, CD45, Nestin, CD146 and CD117 at passage 0. Flow cytometric histographs are representative of triplicate experiments.

transendocardial, intramyocardial or intracoronary cell delivery).

Figure 14 summarizes the key findings [changes in mean LVEF and mean relative amount of scar volume of the left ventricular wall (ScVol) from baseline (*i.e.*, immediately before delivery of cells or control treatment, respectively) to follow-up] from the present study and from all studies on cell therapy for CMI using porcine models that were published so far[38-42] (details of these studies are provided in Table 2). The animals had on average the lowest mean LVEF and the highest mean ScVol at baseline in our study, indicating high clinical relevance. In fact, four[39-42] out of the six studies summarized in Figure 14 investigated porcine models for the study of CMI with moderately reduced LVEF according to a previous study[36], whereas an earlier study by Johnston *et al*[38] as well as ours investigated porcine models for the study of CMI with reduced LVEF[36]. Furthermore, the animals showed the highest increase in mean LVEF and the second-highest reduction in mean ScVol in our study. The mean ScVol was reduced from 19.2% at baseline to 14.2% 8 wk later[38], compared to 20.9% at baseline and 16.6% 6 wk later in our study. Dissimilar to our study, however, no improvement of mean LVEF was found in a former study[38] (37.8% at baseline *vs* 37.6% 8 wk later, compared to 34.3% at baseline *vs* 40.4% 6 wk later in our study).

Analysis of regional replacement fibrosis demonstrated that the reduction in ScVol observed in our study predominantly took place in those left ventricular segments that are assigned to the vascular territory of the LAD in the human heart. Considering that the pattern of coronary arteries and distribution of blood supply in the porcine heart is remarkably similar to that in the human heart[16], these regional replacement fibrosis data support the effectiveness of our therapeutic approach. As indicated in Figure 14, the differences in the outcome between our study and other published studies on cell therapy for CMI using porcine models[38-42] cannot be explained by substantial differences in the time between MI induction and the delivery of cells, or

Table 1 Results of statistical analysis

Parameter	Group 1 (delivery of UA-ADRCs)				Group 2 (delivery of saline as control)				*P* values of repeated measures two-way analysis of variance			
	T1		T2		T1		T2					
	Mean	SEM	Mean	SEM	Mean	SEM	Mean	SEM	I	Time	Tr	SM
LVEF	343	289	404	264	378	257	362	245	0.036	0.207	0.912	0.006
CO	273	022	378	023	339	030	363	032	0.049	0.004	0.458	0.019
SV	314	202	443	239	346	299	380	343	0.036	0.001	0.638	0.048
EDV	936	507	1119	624	926	645	1061	717	0.358	< 0.001	0.696	< 0.001
ESV	621	528	676	649	580	524	681	603	0.327	0.005	0.821	< 0.001
HR	870	293	854	419	974	396	955	361	0.940	0.400	0.051	0001
M_{LV}	553	499	713	449	632	335	684	397	0.042	0.001	0.665	0.001
ScVol	209	229	166	119	176	138	227	176	0.002	0.739	0.509	0.019

The time points T1 and T2 are explained in detail in the main text. *P* values < 0.05 are given boldface. T1: Delivery of UA-ADRCs (group 1) or saline (group 2) 4 wk after induction of myocardial infarction; T2, 6 wk after T1 (*i.e.* 10 wk after induction of myocardial infarction); LVEF: Left ventricular ejection fraction (%) (primary objective); CO: Cardiac output (L/min); SV: Stroke volume (mL); EDV: End diastolic volume (mL); ESV: End systolic volume (mL); HR: Heart rate (min^{-1}); M_{LV}: Left ventricular mass (g); ScVol: Relative amount of scar volume of the left ventricular wall (%); I: Interaction; Tr: Treatment; SM: Subject matching; UA-ADRCs: Fresh, uncultured, unmodified autologous adipose-derived regenerative cells.

the time between the delivery of cells and follow-up. Rather, the differences in outcomes were most probably caused by differences in the type of cells delivered and the delivery route. In fact, in all other studies listed in Figure 14[38-42], allogeneic cells were used [cardiosphere-derived cells (CDCs) in[38-40], adipose-derived stem cells (ASCs) in[41], and a combination of bone marrow-derived stem cells (BMSCs) and allogeneic, c-Kit-positive cardiac stem cells (CSCs)[42]]. Allogeneic ASCs and BMSCs indicated benefits in the treatment of porcine and sheep models for the study of acute MI (delivery of cells immediately after[43-45] or within the first 8 d[46] after induction of MI). However, both the aforementioned studies employing porcine models for the study of CMI[38-42] as well as a recent clinical trial on treatment of CMI with allogeneic ASCs[10] revealed relatively poor outcomes (on average between -0.5% and +1.9% absolute change or between -1.0% and +4.6% relative change in mean LVEF at follow-up in the studies on porcine models[38-42], and on average +2.9% absolute change or +10% relative change in mean LVEF at 6-mo follow-up in the clinical trial[10]). This is significantly less than the average +6.1% absolute change or +17.9% relative change in the mean LVEF reported in the present study. As previously mentioned above, the long-term ability of allogeneic stem cells to preserve function in the treatment of CMI may be limited by an immune response, whereby the allogeneic cells change from an immunoprivileged to an immunogenic state after differentiation[9]. In fact, 40% of the IHD patients enrolled in the clinical trial on treatment of CMI with allogeneic ASCs[10] developed donor-specific *de novo* human leukocyte antigen (HLA) class I antibodies, and 20% of the IHD patients already had donor-specific HLA antibodies at baseline[10]. Using porcine models, Tseliou *et al*[40] found serum alloantibodies only in one out of eight animals 4 wk after delivery of allogeneic CDCs, whereas the other studies[38,39,41,42] did not investigate the development of serum alloantibodies. Natsumeda *et al*[42] occasionally detected inflammatory cells in myocardial tissue 3 mo after delivery of allogeneic BMSCs and CSCs, but attributed this finding to CMI. Blásquez *et al*[39] investigated various immunological parameters 4 wk after the delivery of allogeneic CDCs, and concluded that the observed changes could exert a modulation in the inflammatory environment of the heart in CMI, indirectly benefiting endogenous cardiac repair. However, because of the lack of a control group in the study by Blásquez *et al*[39], this conclusion might be treated with caution.

Nonetheless, it would not be correct to conclude that therapies based on allogeneic cells are in principle less efficient than therapies based on autologous cells for treatment of chronic cardiac failure. Rather, a recent randomized clinical trial (RCT) on patients who suffered from chronic nonischemic dilated cardiomyopathy (NIDCM) who averaged more than 6 years with mean LVEF of approximately 26% at baseline (POSEIDON-DCM)[47] reported improvement of LVEF by averaged +8.0% absolute change 1 year after transendocardial delivery of 100×10^6 allogeneic BMSCs (P = 0.004 compared to baseline), compared to improvement of LVEF who averaged +5.4% absolute change 1 year after transendocardial delivery of 100×10^6 autologous BMSCs (P = 0.116 compared to baseline). The authors of the POSEIDON-DCM RCT[47] hypothesized that the following reasons could explain the better outcome after

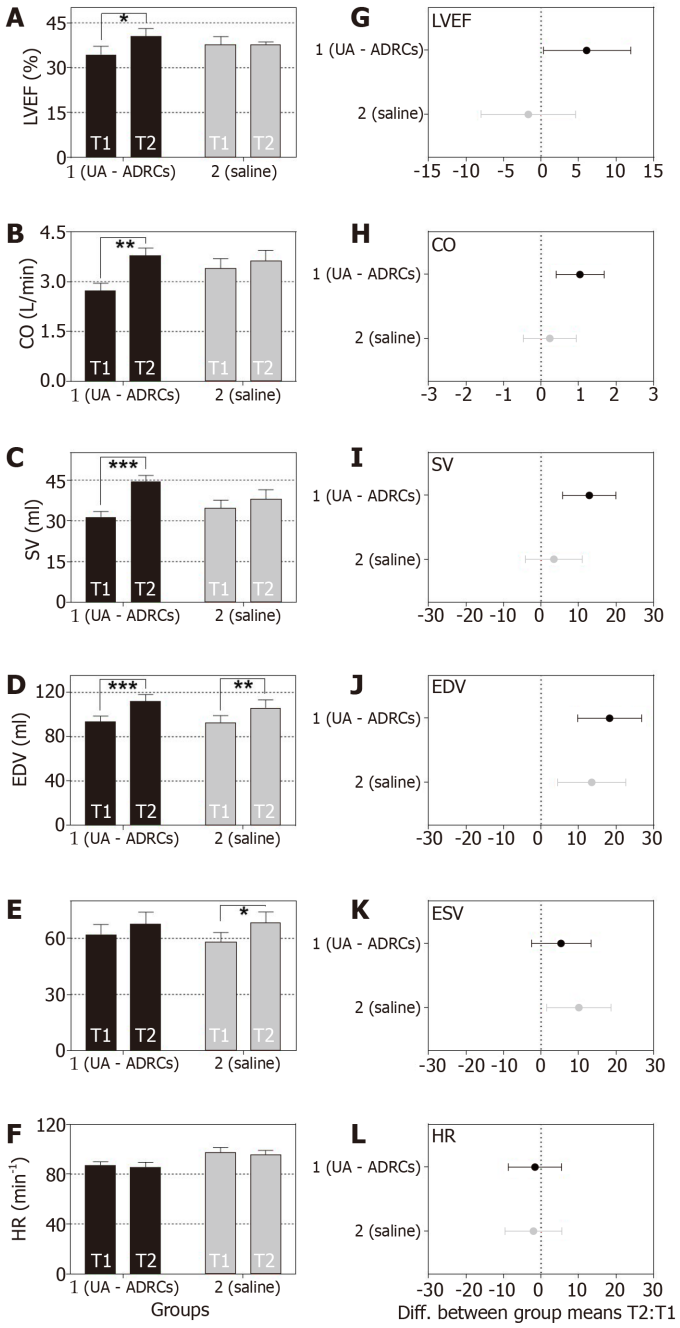

Figure 8 Change in cardiac function after delivery of UA-ADRCs or saline. The panels show group-specific mean ± SE of (A) left ventricular ejection fraction (LVEF, (B) cardiac output (CO), (C) stroke volume (SV), (D) end-diastolic volume (EDV), (E) end-systolic volume (ESV) and (F) heart rate (HR) of animals in group 1 (delivery of UA-ADRCs) (green bars) and group 2 (delivery of saline as control) (red bars) at 4 wk after infarction (T1) and 6 wk later (T2). *P* values of repeated measures two-way analysis of variance are provided in Table 1; results of group-specific Bonferroni's multiple comparison tests are indicated ($^{a}P < 0.05$; $^{b}P < 0.01$; $^{c}P < 0.001$). 95% confidence intervals (Bonferroni) of the differences of group-specific mean data between T2 and T1 are shown in (G-L). UA-ADRCs: Fresh, uncultured, unmodified, autologous adipose-derived regenerative cells.

delivery of allogeneic BMSCs than after delivery of autologous BMSCs: Different mean age of the donors (the donors in the allogeneic BMSC group were on average approximately half as old as the donors in the autologous BMSC group; mean age of the latter: approximately 57.4 years), possible adverse impact of the disease milieu (including the proinflammatory phenotype), and the possibility of enhanced endogenous cardio-repair after delivery of allogeneic BMSCs in chronic NIDCM. However, specific data supporting these hypotheses were not provided in this study[47]. At least the age of the donors itself may not explain the different clinical outcome in the POSEIDON-DCM RCT[47]. A recent study showed that protein expression profiles of human umbilical vein endothelial cells (HUVECs) that were co-

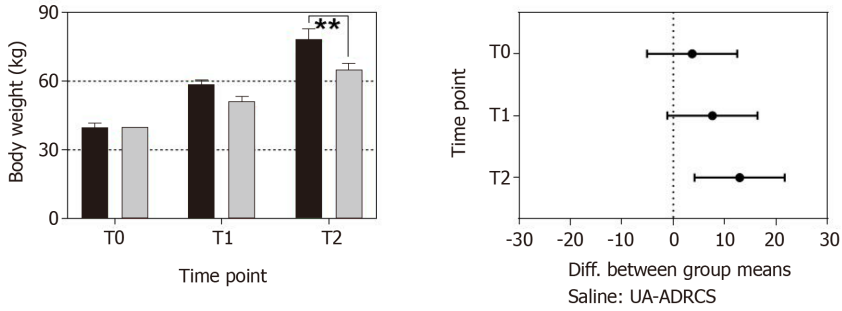

Figure 9 Change in body weight after delivery of UA-ADRCs or saline. The left panel shows group-specific mean ± SE of the body weight of animals in group 1 (delivery of UA-ADRCs) (green bars) and group 2 (delivery of saline as control) (red bars) at baseline (T0), 4 wk after infarction (T1) and 6 wk later (T2). In both groups, the mean body weight significantly increased during the investigated period (group 1: +48% from T0 to T1 and +97% from T0 to T2; group 2: +42% from T0 to T1 and +81% from T0 to T2; $P_{\text{Interaction}} = 0.076$; $P_{\text{Time}} < 0.001$; $P_{\text{Treatment}} = 0.009$; $P_{\text{Subjects (matching)}} = 0.007$). Post hoc Bonferroni tests for pairwise comparisons demonstrated a significant difference in mean body weight between the groups at T2 ($^{b}P < 0.01$) but not at T0 or T1. 95% confidence intervals (Bonferroni) of the differences of group-specific mean data are displayed in the right panel. UA-ADRCs: Fresh, uncultured, unmodified, autologous adipose-derived regenerative cells.

cultured under oxidative stress conditions with UA-ADRCs from healthy persons aged between 42 and 47 years did not differ from protein expression profiles of HUVECs that were co-cultured under identical conditions with ADRCs from healthy persons aged between 61 and 62 years[48]. Nevertheless, one might speculate that the cardiac repair potential of BMSCs obtained from patients suffering from NIDCM for several years (with a reduction in LVEF by more than 50% compared to healthy people[36,49] could differ significantly from the cardiac repair potential of BMSCs obtained from young, healthy people. In any case, the outcome of the POSEIDON-DCM RCT[47] cannot be directly compared to the outcome of treatment of induced chronic MI in porcine animal models (Figure 14). In fact, a RCT on patients who have suffered from chronic IHD with an averaged time of approximately 11 years since the last MI and mean LVEF of approximately 27% at baseline (POSEIDON)[50] reported almost no improvement of LVEF 13 mo after transendocardial delivery of up to 200 × 10^6 allogeneic BMSCs (averaged +1.7% absolute change compared to baseline) or up to 200 × 10^6 autologous BMSCs (averaged +2.3% absolute change compared to baseline). The disappointing outcome of the autologous BMSC group in the POSEIDON RCT[50] may be due to the considerably prolonged time between the last MI and the delivery of cells (on average 12.8 years; range: 2.4-31.8), which may be clinically less relevant than the time between induced MI and the delivery of UA-ADRCs investigated in the present study (4 wk).

Several cell delivery routes were tested in preclinical studies and clinical trials in order to optimize the efficacy of mesenchymal stem cell therapy for MI[51]. A recent meta-analysis of these studies indicated that transendocardial stem cell injection (TESI) may be superior to intramyocardial (transpericardial) injection, intracoronary infusion or intravenous infusion[51]. However, TESI may preferentially reduce scar size and functional response of the ventricular wall at local stem cell injection sites, as observed in the POSEIDON RCT[52]. Thus, TESI might not be the best cell delivery route.

In order to overcome the natural endothelial barrier, we applied in the present study a novel cell delivery method by applying increased pressure to extravasate the cells (retrograde delivery of cells into the temporarily blocked LAD vein using a standard over-the-wire balloon catheter). Another published study on pigs (occlusion of the LAD artery for 45 min; delivery of 1 × 10^7 ^{111}indium-oxine–labeled autologous ASCs 6 d later; delivery of the cells into a 4 cm long segment of the LAD vein using a double-balloon catheter within on average 8 seconds; named RCV delivery) showed that RCV delivery also resulted in increased amounts of cells retained in the heart at 1 h and 24 h after delivery (mean relative amount of ^{111}indium-oxine retention: 18% after 1 h and 19% after 24 h)[53]. Of note, these data cannot be directly compared to the experimental model investigated in the present study (occlusion of the LAD artery for 180 min; delivery of UA-ARDCs 4 wk later). We hypothesize that delivery of cells into a temporarily blocked vessel – with continuing injection and the resulting increase in pressure in the compartment between the balloons blocked segment of the vessel and the capillaries – enables cells to overcome the endothelial barrier. It might be a task of

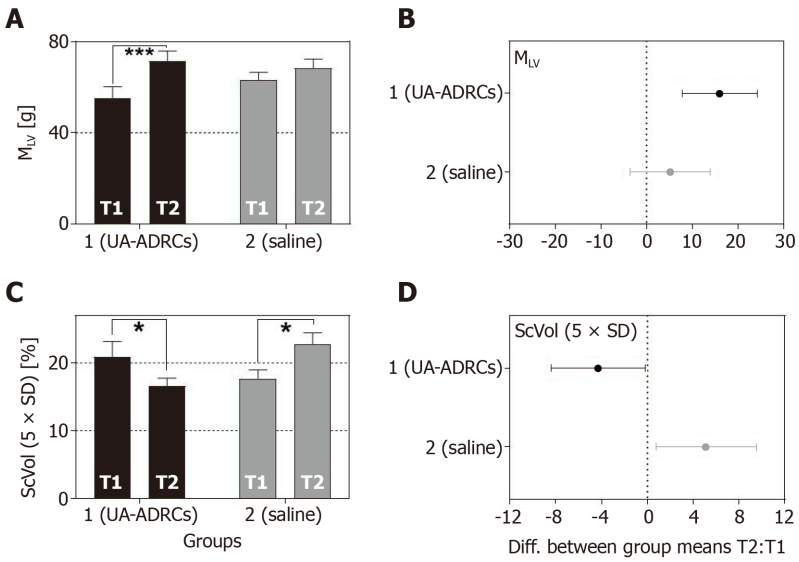

Figure 10 Change in cardiac structure after delivery of UA-ADRCs or saline. The panels show group-specific mean ± SE of (A) the left ventricular mass (M_{LV}) and (B) the relative amount of scar volume of the left ventricular wall (ScVol) of animals in group 1 (delivery of UA-ADRCs) (green bars) and group 2 (delivery of saline as control) (red bars) at 4 wk after infarction (T1) and 6 wk later (T2). *P* values of repeated measures two-way analysis of variance are provided in **Table 1**; results of group-specific Bonferroni's multiple comparison tests are indicated ([a]*P* < 0.05; [c]*P* < 0.001). 95% confidence intervals (Bonferroni) of the differences of group-specific mean data between T2 and T1 are shown in (C, D). UA-ADRCs: Fresh, uncultured, unmodified, autologous adipose-derived regenerative cells.

following studies to further investigate to which extent the novel delivery mode contributed to improvements in cardiac function and structure after induced CMI, as reported here.

The outcome of cell-based therapy for MI depends on the type of cells delivered, which includes the primary origin, way of initial isolation, and processing. The UA-ADRCs used in the present study were neither cultured nor selected or physically, chemically and/or genetically modified. Rather, they were delivered into the heart about one hour after isolating the unmodified cells from the adipose tissue, within the same interventional procedure of cell harvesting and application (*i.e.*, at "point of care").

A number of enzymatic and non-enzymatic systems for isolating UA-ADRCs have been developed[21,54]. The cell yield reported after different procedures varies considerably[21,55]. It was shown that, in general, enzymatic isolation of UA-ADRCs yields significantly more cells than non-enzymatic, mere mechanical isolation[21,56]. In the present study, cells were isolated from adipose tissue using Matrase™ Reagent (InGeneron), an enzyme blend of collagenase I, collagenase II and a recombinantly produced, proprietary neutral protease.

A recent study compared cell yield, cell viability, number of living cells per ml lipoaspirate, biological characteristics, physiological functions and structural properties of UA-ADRCs that were isolated from adipose tissue with the use of Matrase Reagent (Transpose RT/Matrase isolation) (as done in this study) with the same parameters of UA-ADRCs that were mechanically isolated from adipose tissue without the use of Matrase Reagent, but under otherwise identical processing conditions (Transpose RT/no Matrase isolation)[21]. It turned out that, compared to Transpose RT/no Matrase isolation, Transpose RT/Matrase isolation resulted in the following significantly different ($P < 0.05$), clinically relevant effects: (1) An approximately twelve times higher mean number of viable cells per gram processed lipoaspirate; and (2) An approximately 16 times higher number of CFU-Fs per gram lipoaspirate created by the UA-ADRCs[21]. On the other hand, Transpose RT/Matrase isolated UA-ADRCs and Transpose RT/no Matrase isolated UA-ADRCs showed similar, not significantly different ($P > 0.05$) expression levels of the regenerative cell-associated genes Oct4, Hes1 and Klf4[21]. Furthermore, when stimulated with specific differentiation media both Transpose RT / Matrase isolated UA-ADRCs and Transpose RT/no Matrase isolated UA-ADRCs were independently able to differentiate into adipogenic, osteogenic, hepatogenic and neurogenic lineages (*i.e.*, into cells of all three germ layers)[21]. These data demonstrate that (1) the use of Matrase Reagent in isolating UA-ADRCs from adipose tissue did not change

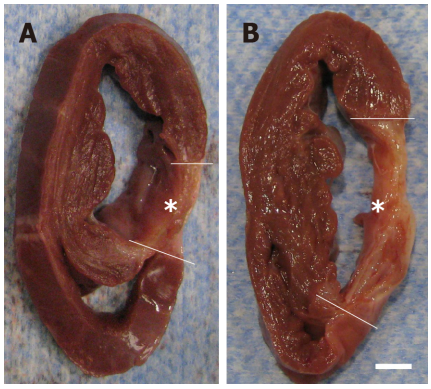

Figure 11 Formation of scar tissue after delivery of UA-ADRCs or saline. A, B: Representative, transversal, 1 cm-thick slices of post mortem hearts from pigs in group 1 (delivery of fresh, uncultured, unmodified, autologous adipose-derived regenerative cells) (A) and group 2 (delivery of saline as control) (B) at T2. The yellow lines indicate the left ventricular border zones of the myocardial infarction (yellow asterisks). The scale bar represents 1 cm. UA-ADRCs: Fresh, uncultured, unmodified, autologous adipose-derived regenerative cells.

biological characteristics, physiological functions or structural properties of the cells that are of relevance for the intended use (*i.e.*, regeneration, repair or replacement of weakened or injured tissue); (2) the Matrase Reagent did not induce these biological characteristics, physiological functions and structural properties; and (3) the cells were not manipulated by the use of the enzyme, because Transpose RT/Matrase isolated UA-ADRCs and Transpose RT/no Matrase isolated UA-ADRCs showed the same expression of embryonic genes and pluripotent differentiation capacity[21]. These data are highly clinically significant, because safety concerns have recently been raised about the use of cultured adult stem cells in regenerative medicine. In particular, increased rates of potential malignant transformations were observed at higher passages[57-59].

Characterization of cells in this study with flow cytometry yielded the following results. First, 49% of the cells on average expressed CD29 ($CD29^+$), and 37% expressed CD44. Expression of CD29 and CD44 is characteristic of UA-ADRCs[55,60]. With regard to CD29, Mitchell *et al*[61] reported similar results for human UA-ADRCs (mean relative number of $CD29^+$ cells: 48%). In contrast, these authors reported higher mean relative numbers of $CD44^+$ cells than those found in this study (64% *vs* 37%). A potential explanation for this discrepancy may be species-specific differences in the expression of CD44. When culturing UA-ADRCs, Mitchell *et al*[61] observed that the mean relative number of $CD29^+$ cells increased from 71% at passage 1 to 95% at passage 4, and the mean relative number of $CD44^+$ cells increased from 84% at passage 1 to 98% at passage 4. Second, the average number of cells in this study that expressed CD45 (a marker of blood-derived cells[55,62]) was only 9%. Of note, substantially higher mean relative numbers of $CD45^+$ cells were reported for porcine UA-ADRCS (31%[13]) and human UA-ADRCS (30%[61,63]) in the literature. A potential explanation is that no Transpose/Matrase isolation of UA-ADRCs was performed in the latter studies[13,61,63]), further underscoring the superiority of the approach used in this study. Third, the average number of cells in this study that expressed CD31 (a marker of endothelial cells[55,63]) was 11%. A very similar average number of $CD31^+$ cells (8%) was previously reported for porcine UA-ADRCs[13]. In contrast, for human UA-ADRCs, conflicting relative numbers of $CD31^+$ cells were reported in the literature (1%-6% in [63], and 22% on average in[61]). A potential explanation is the use of different isolation procedures in these studies. Fourth, the average number of cells in this study that expressed Oct4 (a transcription factor expressed in human ASCs at passage 1 and is highly associated with stem cell pluripotency[64]) was 4%. Of note, this number could not be compared to results from the other studies discussed here[13,55,60-63] because Oct4 was not investigated in these studies. Fifth, the relative numbers of cells in this study that expressed NG2 and CD146 (which were described in the literature as markers associated with pericytes[55,65]), Nestin (an early marker of neural stem/progenitor cells and proliferative endothelial cells[66]) and CD117 (c-Kit; a marker of common myeloid progenitors, hematopoietic progenitor cells and multipotent progenitors[67]) were 10%, 1%, 4% and 0.3%, respectively. These markers were not investigated in the aforementioned study on UA-ADRCs[13]. Mitchell *et al*[61] only reported an average relative number of 21% of $CD146^+$ cells in human UA-ADRCs. Potential explanations of this discrepancy (1% in this study *vs* 21% in[61]) are species-specific differences, differences in the isolation procedure of UA-ADRCs, or a

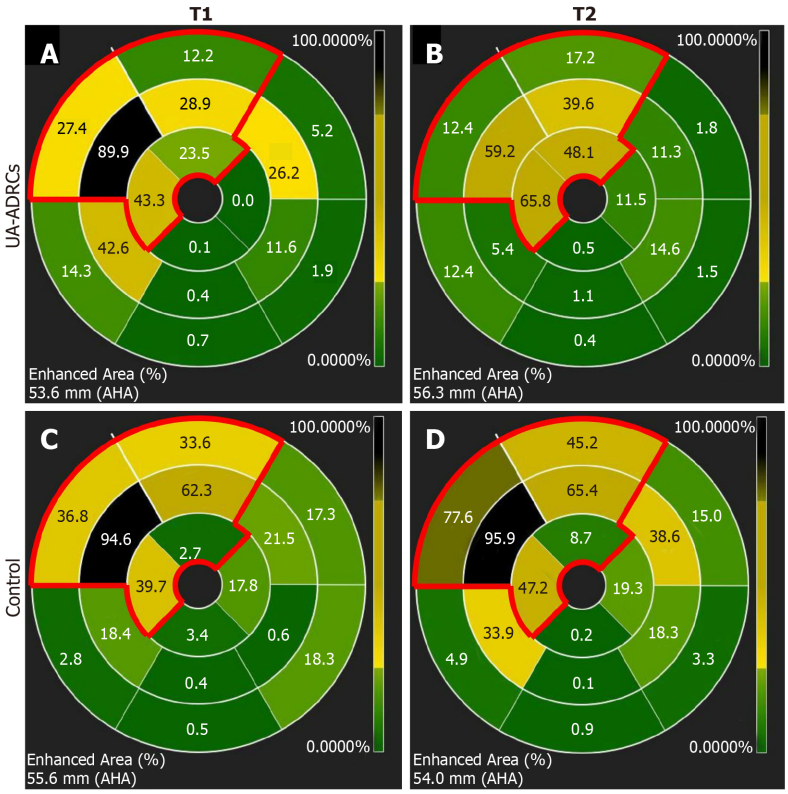

Figure 12 Analysis of regional replacement fibrosis after delivery of UA-ADRCs or saline. The panels visualize data from a representative animal in group 1 (delivery of UA-ADRCs) (A, B) and a representative animal in group 2 (delivery of saline as control) (C, D) at time points T1 (A, C) and T2 (B, D) using color-coded, AHA 17-segment bullseye plots[35]. Segments marked green showed viable myocardium, whereas segments marked black showed complete fibrosis (*i.e.* $NPrel_{SI>5SD}$ > 90%; see main text for details). In all panels, the red lines in the upper left parts of the bullseye plots enclose those segments that are assigned to the territory of the left anterior descending artery in the human heart[35]. The asterisks indicate the mid anteroseptal segment #8 that markedly improved between T1 and T2 after delivery of UA-ADRCs (A, B) but not after delivery of saline as control (C, D). UA-ADRCs: Fresh, uncultured, unmodified, autologous adipose-derived regenerative cells.

mixture thereof. Collectively, these data support the significance of the UA-ADRCs used in this study to regenerate cardiac tissue in CMI.

It should be mentioned that characterization of the cells delivered in the present study did not follow recommendations published in a joint position statement by the International Federation for Adipose Therapeutics and Science (IFATS) and the International Society for Cellular Therapy (ISCT) in 2013 regarding SVF and ASCs[30]. In this joint position statement, it was stated that primary stable positive surface markers for stromal cells would be CD13, CD29, CD34 (> 20%), CD44, CD73 and CD90 (> 40%), whereas primary negative surface markers for stromal cells would be CD31 (< 20%) and CD45 (< 50%)[30]. Furthermore, at least 20% of the SVF would contain a stromal cell population that is immunopositive for the surface marker CD34 and immunonegative for the surface markers CD31, CD45 and CD235a (*i.e.*, $CD31^-/CD34^+/CD45^-/CD235a^-$ cells)[30]. This statement was based on an earlier position statement published by ISCT in 2006 that described "being adherent to plastic, expressing the surface markers CD73, CD90 and CD105, and having the ability to differentiate into osteoblasts, adipocytes and chondrocytes[68]" as the minimal criteria for defining MSCs. However, it should be pointed out that a major shortcoming of this definition of multipotent MSCs is the fact that, for example, fibroblasts also adhere to plastic and express the surface markers CD73, CD90 and CD105, without having the ability to transdifferentiate into other lineages or being MSCs[64]. Furthermore, true pluripotent stem cells do not yet express CD73, CD90 and CD105[24]. Besides this, a recent study compiled the relative amount of ADRCs expressing the surface markers CD13, CD29, CD34, CD44, CD73, CD90, CD31 and CD45, as reported in all studies describing enzymatic and non-enzymatic methods for isolating ADRCs that were published so far[24]. In brief, it was found that (1) the relative amount of $CD34^+$ cells was determined for only very few methods, with substantial variation among methods (ranging between 35%-81%); (2) the relative amount of $CD45^+$ cells varied between 6%-82% among published studies; (3) relative

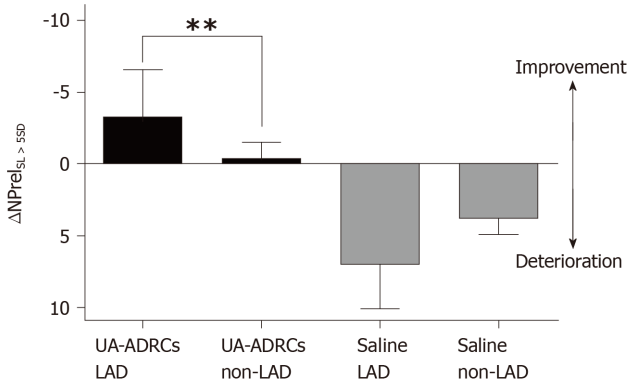

Figure 13 Improvement or deterioration of regional replacement fibrosis after delivery of UA-ADRCs or saline. The panel shows mean and standard error of the mean of the results of replacement fibrosis analysis (as explained in detail in the main text) of segments that are assigned to the territory of the left anterior descending artery in the human heart LAD segments; analysis is also shown for segments that are assigned to the territory of the right coronary artery and the left circumflex coronary artery in the human heart (non-LAD segments) of animals in group 1 [delivery of UA-ADRCs) (green boxes) and group 2 (delivery of saline as control) (red boxes). Data above the zero line indicate improvement, and data below the zero line deterioration. Results of Bonferroni's multiple comparison tests are indicated ($^bP < 0.01$). LAD: Left anterior descending; UA-ADRCs: Fresh, uncultured, unmodified, autologous adipose-derived regenerative cells.

amounts of $CD13^+$ cells, $CD29^+$ cells, $CD44^+$ cells, $CD73^+$ cells, $CD90^+$ cells and $CD31^+$ cells were only determined for a few methods; and (4) the relative amount of $CD31^-/CD34^+/CD45^-/CD235a^-$ cells (as proposed in[30]) was not reported for any method[24]. Collectively, these data render the determination of ADRC surface markers as proposed by IFATS and ISCT[30,68] to not be suitable. This was the reason why no such characterization as proposed by IFATS and ISCT[30,68] was performed in this study.

Unlike cultured cells, UA-ADRCs cannot be labeled. Accordingly, it is more complex to assess the fate of UA-ADRCs after delivery, unlike in the case of allogenic adipose-derived regenerative cells, or in the case of cultured cells that were labeled in culture. Allogenic adipose-derived regenerative cells can be identified in the host tissue using immunohistochemistry[69], and labeled cells can be identified in the host tissue using immunohistochemistry[70], T2* MRI[71] or single-photon emission computed tomography[53]. It is crucial to keep in mind that all this is not possible in the case of UA-ADRCs. It is not possible to collect conditioned medium from UA-ADRCs, nor is it feasible for cultured cells[72]. These factors limit the evaluation of the exact molecular or cellular effects of UA-ADRCs on the therapeutic outcome after MI.

In our study, the delivery of UA-ADRCs in CMI resulted in an increased mean mass of the left ventricle, and a reduced mean relative amount of scar volume of the left ventricular wall (Figures 11-13). In this regard, it is critical to note that in treatments of acute MI, stem cells act *via* different molecular and cellular mechanisms of action than in treatments of chronic MI. In the case of acute MI, the predominant effect of stem cell application may be the prevention of cardiomyocyte apoptosis[73]. However, in our study, delivery of UA-ADRCs into the LAD vein took place 4 wk post-MI. A study on a rat model of MI demonstrated high numbers of active caspase-3 immunopositive (*i.e.*, apoptotic) cells in cardiomyocytes and nonmyocytes at 7-10 d post-MI, but not at 28 d post-MI[8]. Accordingly, in the case of chronic MI, the predominant effect of stem cell application may be the enhancement of the neovascularization response after MI (demonstrated in Figure 5 as well as in[38,40,41]), and the formation of new cardiomyocytes. With regard to the latter, it was a recent key finding that endogenous cardiomyocyte generation can be activated by exercise in the normal and injured adult mouse heart[74]. This obviously does not exclude that the UA-ADRCs applied in this study may also have exerted their function by any (or a combination of several) of the molecular and cellular mechanisms that were described in the literature (such as beneficial effects on the ratio between matrix metalloproteinases and tissue inhibitors of metalloproteinases, reduced collagen expression, inhibited growth of cardiac fibroblasts, and limited local inflammation[75-78]).

Our study has some limitations. One limitation is that only a specific combination of cell type, cell dose, cell delivery route and timing of cell delivery was tested, and this was performed in a pre-determined location of CMI with uniform infarct size. However, it turned out that this specific combination of cell type, dose, delivery route

Table 2 Details of studies that addressed delivery of cultured cells (adipose-derived stem cells, bone marrow-derived stem cells, cardiosphere-derived cells, and c-Kit-positive cardiac stem cells) at a later time after experimentally-induced myocardial infarction in porcine models

Ref.	**Johnston *et al*[38]**
Species	Swine (farm and miniature pigs; age and body weight of the animals not provided)
Duration of LAD occlusion	150 min
Cells	CDCs
Source of cells	
No. of cells	300000 cells/kg body weight
Delivery time	4 wk after MI
Delivery route	Intracoronary
Investigated groups of animals	Group B (group 3 in Figure [14]): 300000 cells/kg body weight
	Group A (group 4 in Figure [14]): Control group
Follow-up	8 wk after delivery of cells (12 wk post-MI)
Use of cardiac MRI	Yes (3T; Siemens, Erlangen, Germany)
mLVEF before MI	
mLVEF after MI	37.8% (group A) and 39.5% (group B)
mLVEF at follow-up	37.6% (group A) and 37.0% (group B)
ΔmLVEF (absolute numbers)	-0.2% (group A) and -1.5% (group B)
ΔmLVEF (relative numbers)	-0.5% (group A) and -6.3% (group B)
mScVol after MI	19.2% (group A) and 17.7% (group B)
mScVol at follow-up	14.2% (group A) and 15.3% (group B)
ΔmScVol (absolute numbers)	-5.0% (group A) and -2.4% (group B)
ΔmScVol (relative numbers)	-26.0% (group A) and -13.6% (group B)
Ref.	**Blázquez *et al*[39]**
Species	Large white pigs (3-4 mo old; body weight 30-35 kg)
Duration of LAD occlusion	90 min
Cells	Allogeneic CDCs
Source of cells	Large White pigs
No. of cells	300000 cells/kg body weight
Delivery time	7 wk after MI
Delivery route	Intrapericardial injection
Investigated groups of animals	Group A (group 5 in Figure [14]): 300000 cells/kg body weight (n = 4)
Follow-up	4 wk after delivery of cells (11 wk post-MI)
Use of cardiac MRI	Yes (1.5 T; Intera, Philips Medical System, Eindhoven, Netherlands)
mLVEF before MI	
mLVEF after MI	39.4
mLVEF at follow-up (4 wk)	40.2
ΔmLVEF (absolute numbers)	+0.8%
ΔmLVEF (relative numbers)	+2.0%
mScVol after MI	10.2%
mScVol at follow-up	8.7%
ΔmScVol (absolute numbers)	-1.5%
ΔmScVol (relative numbers)	-17.2%
Notes	No control group
Ref.	**Tseliou *et al*[40]**
Species	Female Yucatan mini pigs (body weight 40-45 kg); age of the animals not provided
Duration of LAD occlusion	150 min
Cells	Allogeneic CDCs
Source of cells	Male donor Sinclair pigs
No. of cells	12.5×10^6
Delivery time	3 wk after MI
Delivery route	Intracoronary

Investigated groups of animals	Group A: Single-vessel LAD arterial infusion under stop-flow (n = 5)
	Group B: Single-vessel LAD arterial infusion under continuous flow (n = 5)
	Group C: Multi-vessel control group (n = 5)
	Group D: Multi-vessel (LAD, LCX and RCA) under stop-flow (n = 5)
	Group E (group 6 in Figure [14]): Multi-vessel (LAD, LCX and RCA) under continuous flow (n = 6)
	Group F (group 7 in Figure [14]): Control group (n = 5)
Follow-up	7 wk after delivery of cells (4 wk post-MI)
Use of cardiac MRI	Yes (3T; Siemens, Erlangen, Germany)
mLVEF before MI	
mLVEF after MI	47.7% (group A), 43.5% (group B), 46.2% (group C), 48.1% (group D) and 47.4% (group E) and 44.8% (group F)
mLVEF at follow-up	44.9% (group A), 41.6% (group B), 40.3% (group C), 45.6% (group D) and 46.9% (group E) and 37.9% (group F)
ΔmLVEF (absolute numbers)	-2.76% (group A), -1.9% (group B), -5.9% (group C), -2.4% (group D) and -0.5% (group E) and -6.9% (group F)
ΔmLVEF (relative numbers)	-6.1% (group A), -4.5% (group B), -14.5% (group C), -5.3% (group D) and -1.0% (group E) and -18.3% (group F)
mScVol after MI	17.1% (group A), 17.0% (group B), 17.6% (group C), 15.8% (group D) and 14.6% (group E) and 16.0% (group F)
mScVol at follow-up	14.7% (group A), 15.9% (group B), 14.2% (group C), 11.4% (group D) and 11.9% (group E) and 12.1% (group F)
ΔmScVol (absolute numbers)	-2.4% (group A), -1.1% (group B), -3.4% (group C), -4.4% (group D) and -2.7% (group F) and -3.9% (group F)
ΔmScVol (relative numbers)	-16.4% (group A), -6.9% (group B), -24.1% (group C), -38.1% (group D) and -22.5% (group E) and -31.8% (group F)
Ref.	**Dariolli *et al*[41]**
Species	Female *Sus scrofa domestica* pigs (body weight 15-20 kg); age of the animals not provided
Duration of LCX occlusion	Permanent occlusion
Cells	Allogeneic ASCs (passage 4)
Source of cells	Not provided
No. of cells	Between 1×10^6 and 4×10^6
Delivery time	4 wk after MI
Delivery route	Transpericardial intramyocardial injection (20 different sites around the border of MI)
Investigated groups of animals	Group A: 1×10^6 cells/kg body weight (n = 6)
	Group B: 2×10^6 cells/kg body weight (n = 7)
	Group C (group 8 in Figure [14]): 4×10^6 cells/kg body weight (n = 5)
	Group D (group 9 in Figure [14]): Control group (n = 7)
Follow-up	4 wk after delivery of cells (8 wk post-MI)
Use of cardiac MRI	No
mLVEF before MI	
mLVEF after MI	48.4% (group A), 46.7% (group B), 48.7% (group C) and 44.9% (group D)
mLVEF at follow-up	40.6% (group A), 42.2% (group B), 50.0% (group C) and 35.9% (group D)
ΔmLVEF (absolute numbers)	-8.2% (group A), -4.5% (group B), +1.3% (group C) and -9.0% (group D)
ΔmLVEF (relative numbers)	-20.2% (group A), -10.7% (group B), +2.6% (group C) and -25.1% (group D),
mScVol after MI	Not provided
mScVol at follow-up	Not provided
ΔmScVol (absolute numbers)	Not provided
ΔmScVol (relative numbers)	Not provided
Notes	Measurements of LVEF were performed with echocardiography
Ref.	**Natsumeda *et al*[42]**
Species	Female Göttingen swine; age and body weight of the animals not provided
Duration of LAD occlusion	150 min
Cells	Allogeneic BMSCs and allogeneic CSCs
Source of cells	Male Yorkshire swine
No. of cells	Between 1×10^6 and 2×10^8
Delivery time	3 mo after MI

Delivery route	Transendomyocardial intramyocardial injection (TESI) 10 different sites around the border of MI
Investigated groups of animals	Group A: 2×10^8 BMSCs (n = 8)
	Group B: 1×10^6 CSCs (n = 4)
	Group C (group 10 in Figure [14]): 1×10^6 CSCs + 2×10^8 BMSCs (n = 7)
	Group D (group 11 in Figure [14]): Control group (n = 6)
Follow-up	3 mo after delivery of cells (6 mo post-MI)
Use of cardiac MRI	Yes (3T; TIM Trio; Siemens, Erlangen, Germany)
mLVEF before MI	55.3% (group A), 55.2% (group B), 53.8% (group C) and 57.7% (group D)
mLVEF after MI	37.1% (group A), 43.3% (group B), 39.7% (group C) and 41.7% (group D)
mLVEF at follow-up	36.5% (group A), 43.1% (group B), 41.6% (group C) and 40.7% (group D)
ΔmLVEF (absolute numbers)	-0.6% (group A), -0.2% (group B), +1.9% (group C) and -1.0% (group D)
ΔmLVEF (relative numbers)	-1.6%(group A), -0.5% (group B), +4.6% (group C) and -2.5% (group D)
mScVol after MI	16.9% (group A), 12.8% (group B),15.5% (group C) and 17.5% (group D)
mScVol at follow-up	13.7% (group A), 12.4% (group B), 12.5% (group C) and 19.9% (group D)
ΔmScVol (absolute numbers)	-3.2% (group A), -0.4% (group B), -3.0% (group C) and +2.4% (group D)
ΔmScVol (relative numbers)	-23.4% (group A), -3.2% (group B), -24.0% (group C) and +12.1% (group D)

Unlike in the present study, Johnston *et al*[38] identified hyper-enhancement as areas of signal intensity > 2 standard deviations greater than normal myocardium (> 5 standard deviations in the present study). LAD: Left anterior descending artery; LCX: Left circumflex artery; mLVEF: Mean left ventricular ejection fraction; MI: Myocardial infarction; mScVol: Mean relative amount of scar volume of the left ventricular wall.

and timing outperformed the state-of-the-art (Figure 14), highlighting the significance of the results presented in this study. Another limitation is that we did not determine aggregate numbers of cardiomyocytes, which is the only way to unequivocally determine whether a certain therapy increased the number of cardiomyocytes in MI/IHD. The design-based stereologic "optical fractionator" is the state-of-the-art methodology for determining total numbers of cells in an organ[79], and determination of total numbers of cardiomyocytes using the optical fractionator was conclusively demonstrated in the literature[80]. However, to our knowledge, studies on cell-based therapies for MI in which total numbers of cardiomyocytes were investigated using design-based stereology have not yet been published, which is most likely due to the complexity of the necessary histologic analyses. The same applies to the analysis of microvessel density and network complexity as a function of the distance to the myocardial infarction zone, as well as to the determination of proliferating cells (both endogenous and delivered ones) and the quantification of numbers of delivered cells that have differentiated into either cardiomyocytes or cells in vessel walls (the latter requiring analysis of both absolute and relative numbers, related to the total number of cardiomyocytes and the number of cells participating in the formation of vessel walls). Development of adequate methods in quantitative histology/design-based stereology are currently underway, and will allow such studies to be reported in the foreseeable future.

In conclusion, the present study indicates that the delivery of UA-ADRCs by a balloon-blocked retrograde venous injection 4 wk after MI is effective, producing a significant increase in cardiac output and significant reduction in the relative amount of scar volume of the left ventricular wall, without adverse effects occurring during the observation period. Our results could trigger further studies relating to: Evaluation of different doses, delivery route, and timing of UA-ADRCs for treating CMI (including the isolation procedure used) as presented here in future clinical trials under strict criteria, as recently suggested[17].

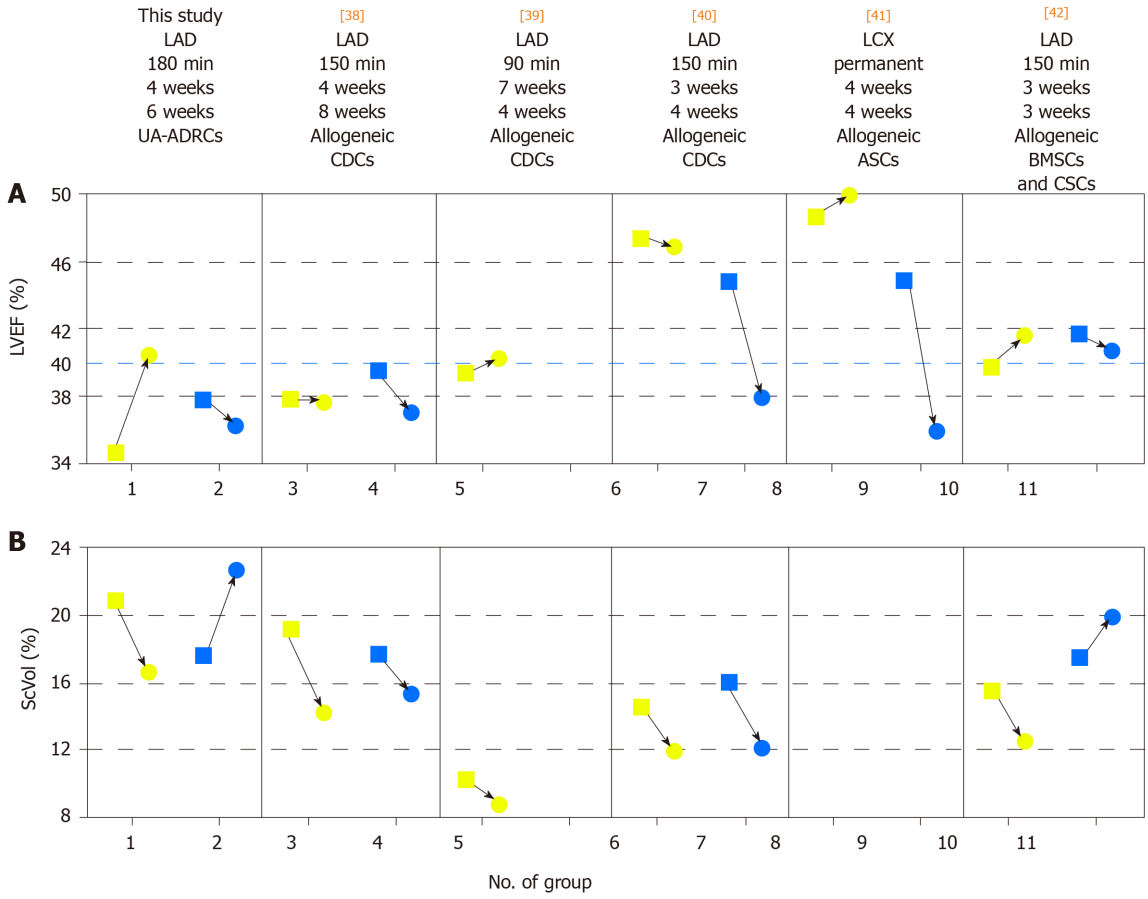

Figure 14 Comparison of studies on cell therapy for chronic MI using porcine models. A, B: Change in mean left ventricular ejection volume (LVEF) (A) and mean relative amount of scar volume of the left ventricular wall (ScVol) (B) from the time immediately before delivery of cells (yellow squares; groups 1, 3, 5, 6, 8 and 10) or control treatment (blue squares; groups 2. 4. 7, 9 and 11), respectively, to follow-up (yellow and blue dots) in the present study (groups 1 and 2) and in all studies on cell therapy for chronic myocardial infarction (> 4 wk) using porcine models that were published to date (groups 3-11; specified in detail in **Table 2**; note that no control group was investigated in[39]). If more than one cell therapy was tested in a study (**Table 2**), the results of the therapy with the most satisfactory outcome are displayed. The information provided on top of Panel A specifies the number of the study in the reference list, the coronary artery that was occluded for experimental MI induction, the duration of occlusion, the interval between experimental MI induction and delivery of cells, and the delivered cell types. The dotted blue line in (A) indicates the border between a moderately reduced LVEF and a reduced LVEF, according to the guidelines for the diagnosis and treatment of acute and chronic heart failure published by the European Society of Cardiology in 2016[36]. MI: Myocardial infarctions; LAD: Left anterior descending artery; LCX: Left circumflex artery; BMSCs: Bone marrow-derived stem cells; CDCs: Cardiosphere-derived stem cells; ASCs: Adipose-derived stem cells; CSCs: Cardiac stem cells; UA-ADRCs: Fresh, uncultured, unmodified autologous adipose-derived regenerative cells.

ARTICLE HIGHLIGHTS

Research background

Cardiovascular diseases substantially contribute to morbidity and mortality worldwide. Myocardial infarction (MI) is one of the most common consequences of ischemic heart disease. Advanced medical treatments and device-based therapies have substantially improved the survival of patients with MI. However, these therapies can only rescue the remaining viable myocardial tissue within the damaged heart, but cannot replace lost myocardium. Accordingly, numerous studies have investigated cell-based therapies for MI. The conflicting results of these studies have established the need for developing innovative approaches for applying cell-based therapy for MI.

Research motivation

Experimental studies on animal models (performed by ourselves and others) demonstrated the potential of fresh, uncultured, unmodified, autologous adipose-derived regenerative cells (UA-ADRCs) for treating acute MI. In contrast, studies on the treatment of chronic MI (CMI; > 4 wk post-MI) with UA-ADRCs have not been published thus far. Our promising results from treating a porcine model with UA-ADRCs for the study of acute MI (*Int J Cardiol* 2010; 144: 26-35) motivated us to investigate the effectiveness and safety of UA-ADRCs for treating CMI in a porcine model. Besides this, as one of several methods for delivering cells to the myocardium, retrograde delivery into a temporarily blocked coronary vein has recently been demonstrated to be an effective option.

Research objectives
Our study aimed to test (in a porcine model for the study of CMI) the following hypotheses: (1) Occlusion of the left anterior descending (LAD) coronary artery for three hours results in a clinically relevant reduction of the left ventricular ejection fraction (LVEF) to less than 40% on an average of 4 wk post-MI (demonstrating significance of the used animal model); (2) Delivery of UA-ADRCs into the LAD vein 4 wk post-MI in this model leads to improved LVEF by more than 15% (relative change) on an average of 10 wk post-MI (primary objective of this study); and (3) The same animal model shows improvements in cardiac structure 6 wk after the delivery of UA-ADRCs (*i.e*. 10 wk post-MI) (secondary objective of this study).

Research methods
The LAD coronary artery of pigs was blocked for 180 min at time point T0. Then, either 18×10^6 UA-ADRCs prepared at "point of care" or saline as control were retrogradely delivered *via* an over-the-wire balloon catheter placed in the temporarily blocked LAD vein 4 wk after T0 (T1). Effects of cells or saline were assessed by cardiac magnetic resonance (CMR) imaging, late gadolinium enhancement CMR imaging and post mortem histologic analysis 10 wk after T0 (T2).

Research results
Unlike the delivery of saline, the delivery of UA-ADRCs demonstrated statistically significant improvements in cardiac function and structure at T2 compared to T1: increased mean LVEF (UA-ADRCs group: +18%; saline group: -4.2%), increased mean cardiac output (UA-ADRCs group: +41%; saline group: +5.9%), increased mean mass of the left ventricle (UA-ADRCs group: +29%; saline group: +8.2%) and reduced mean relative amount of scar volume of the left ventricular wall (UA-ADRCs group: -21%; saline group: +29%).

Research conclusions
The present study indicates that delivery of UA-ADRCs by a balloon-blocked retrograde venous injection 4 wk after MI is effective, producing a significant increase in cardiac output and significant reduction in the relative amount of scar volume of the left ventricular wall, without adverse effects occurring during the observation period.

Research perspectives
Our results justify the evaluation of a new combination of UA-ADRCs (including the isolation procedure), dose, delivery route and timing presented here in future clinical trials for treating CMI under strict criteria, as recently suggested by the European Society of Cardiology Working Group Cellular Biology of the Heart (*Eur Heart J* 2016; 37: 1789-1798), which includes the use of CMR imaging and clinically-relevant endpoints.

REFERENCES

1 **Anderson JL**, Morrow DA. Acute Myocardial Infarction. *N Engl J Med* 2017; **376**: 2053-2064 [PMID: 28538121 DOI: 10.1056/NEJMra1606915]
2 **Ma T**, Sun J, Zhao Z, Lei W, Chen Y, Wang X, Yang J, Shen Z. A brief review: adipose-derived stem cells and their therapeutic potential in cardiovascular diseases. *Stem Cell Res Ther* 2017; **8**: 124 [PMID: 28583198 DOI: 10.1186/s13287-017-0585-3]
3 **Yu H**, Lu K, Zhu J, Wang J. Stem cell therapy for ischemic heart diseases. *Br Med Bull* 2017; **121**: 135-154 [PMID: 28164211 DOI: 10.1093/bmb/ldw059]
4 **Wu R**, Hu X, Wang J. Concise Review: Optimized Strategies for Stem Cell-Based Therapy in Myocardial Repair: Clinical Translatability and Potential Limitation. *Stem Cells* 2018; **36**: 482-500 [PMID: 29330880 DOI: 10.1002/stem.2778]
5 **Menasché P**. Cell therapy trials for heart regeneration - lessons learned and future directions. *Nat Rev Cardiol* 2018; **15**: 659-671 [PMID: 29743563 DOI: 10.1038/s41569-018-0013-0]
6 **Chen L**, Qin F, Ge M, Shu Q, Xu J. Application of adipose-derived stem cells in heart disease. *J Cardiovasc Transl Res* 2014; **7**: 651-663 [PMID: 25205213 DOI: 10.1007/s12265-014-9585-1]
7 **Blank AC**, van Veen TA, Jonsson MK, Zelen JS, Strengers JL, de Boer TP, van der Heyden MA. Rewiring the heart: stem cell therapy to restore normal cardiac excitability and conduction. *Curr Stem Cell Res Ther* 2009; **4**: 23-33 [PMID: 19149627 DOI: 10.2174/157488809787169066]
8 **Rafatian N**, Westcott KV, White RA, Leenen FH. Cardiac macrophages and apoptosis after myocardial infarction: effects of central MR blockade. *Am J Physiol Regul Integr Comp Physiol* 2014; **307**: R879-R887 [PMID: 25100076 DOI: 10.1152/ajpregu.00075.2014]
9 **Huang XP**, Sun Z, Miyagi Y, McDonald Kinkaid H, Zhang L, Weisel RD, Li RK. Differentiation of allogeneic mesenchymal stem cells induces immunogenicity and limits their long-term benefits for myocardial repair. *Circulation* 2010; **122**: 2419-2429 [PMID: 21098445 DOI: 10.1161/CIRCULATIONAHA.110.955971]
10 **Kastrup J**, Haack-Sørensen M, Juhl M, Harary Søndergaard R, Follin B, Drozd Lund L, Mønsted Johansen E, Ali Qayyum A, Bruun Mathiasen A, Jørgensen E, Helqvist S, Jørgen Elberg J, Bruunsgaard H, Ekblond A. Cryopreserved Off-the-Shelf Allogeneic Adipose-Derived Stromal Cells for Therapy in Patients with Ischemic Heart Disease and Heart Failure-A Safety Study. *Stem Cells Transl Med* 2017; **6**: 1963-1971 [PMID: 28880460 DOI: 10.1002/sctm.17-0040]
11 **Fraser JK**, Wulur I, Alfonso Z, Hedrick MH. Fat tissue: an underappreciated source of stem cells for biotechnology. *Trends Biotechnol* 2006; **24**: 150-154 [PMID: 16488036 DOI: 10.1016/j.tibtech.2006.01.010]
12 **Valina C**, Pinkernell K, Song YH, Bai X, Sadat S, Campeau RJ, Le Jemtel TH, Alt E. Intracoronary administration of autologous adipose tissue-derived stem cells improves left ventricular function, perfusion, and remodelling after acute myocardial infarction. *Eur Heart J* 2007; **28**: 2667-2677 [PMID:

17933755 DOI: 10.1093/eurheartj/ehm426]
13 **Alt E**, Pinkernell K, Scharlau M, Coleman M, Fotuhi P, Nabzdyk C, Matthias N, Gehmert S, Song YH. Effect of freshly isolated autologous tissue resident stromal cells on cardiac function and perfusion following acute myocardial infarction. *Int J Cardiol* 2010; **144**: 26-35 [PMID: 19443059 DOI: 10.1016/j.ijcard.2009.03.124]
14 **van Dijk A**, Naaijkens BA, Jurgens WJ, Nalliah K, Sairras S, van der Pijl RJ, Vo K, Vonk AB, van Rossum AC, Paulus WJ, van Milligen FJ, Niessen HW. Reduction of infarct size by intravenous injection of uncultured adipose derived stromal cells in a rat model is dependent on the time point of application. *Stem Cell Res* 2011; **7**: 219-229 [PMID: 21907165 DOI: 10.1016/j.scr.2011.06.003]
15 **Houtgraaf JH**, den Dekker WK, van Dalen BM, Springeling T, de Jong R, van Geuns RJ, Geleijnse ML, Fernandez-Aviles F, Zijlsta F, Serruys PW, Duckers HJ. First experience in humans using adipose tissue-derived regenerative cells in the treatment of patients with ST-segment elevation myocardial infarction. *J Am Coll Cardiol* 2012; **59**: 539-540 [PMID: 22281257 DOI: 10.1016/j.jacc.2011.09.065]
16 **Weaver ME**, Pantely GA, Bristow JD, Ladley HD. A quantitative study of the anatomy and distribution of coronary arteries in swine in comparison with other animals and man. *Cardiovasc Res* 1986; **20**: 907-917 [PMID: 3802126 DOI: 10.1093/cvr/20.12.907]
17 **Madonna R**, Van Laake LW, Davidson SM, Engel FB, Hausenloy DJ, Lecour S, Leor J, Perrino C, Schulz R, Ytrehus K, Landmesser U, Mummery CL, Janssens S, Willerson J, Eschenhagen T, Ferdinandy P, Sluijter JP. Position Paper of the European Society of Cardiology Working Group Cellular Biology of the Heart: cell-based therapies for myocardial repair and regeneration in ischemic heart disease and heart failure. *Eur Heart J* 2016; **37**: 1789-1798 [PMID: 27055812 DOI: 10.1093/eurheartj/ehw113]
18 **National Research Council**. Division on Earth and Life Studies, Institute for Laboratory Animal Research, Committee for the Update of the Guide for the Care and Use of Laboratory Animals of the National Academies. Guide for the Care and Use of Laboratory Animals. Washington: The National Academies Press 2011;
19 **Rutering J**, Ilmer M, Recio A, Coleman M, Vykoukal J, Alt E. Improved Method for Isolation of Neonatal Rat Cardiomyocytes with Increased Yield of C-Kit+ Cardiac Progenitor Cells. *J Stem Cell Res Ther* 2015; **5**: 1-8 [PMID: 26937295 DOI: 10.4172/2157-7633.1000305]
20 **Metcalf GL**, McClure SR, Hostetter JM, Martinez RF, Wang C. Evaluation of adipose-derived stromal vascular fraction from the lateral tailhead, inguinal region, and mesentery of horses. *Can J Vet Res* 2016; **80**: 294-301 [PMID: 27733784]
21 **Winnier G**, Valenzuela N, Alt C, Alt EU. Isolation of adipose tissue derived regenerative cells from human subcutaneous tissue with or without the use of enzymatic reagent; 2018. Preprint. Available from: bioRxiv 485318. Cited February 17, 2019. [DOI: 10.1101/485318]
22 **Konstantinow A**, Arnold A, Djabali K, Kempf W, Gutermuth J, Fischer T, Biedermann T. Therapy of ulcus cruris of venous and mixed venous arterial origin with autologous, adult, native progenitor cells from subcutaneous adipose tissue: a prospective clinical pilot study. *J Eur Acad Dermatol Venereol* 2017; **31**: 2104-2118 [PMID: 28750144 DOI: 10.1111/jdv.14489]
23 **Solakoglu Ö**, Götz W, Kiessling MC, Alt C, Schmitz C, Alt EU. Improved guided bone regeneration by combined application of unmodified, fresh autologous adipose derived regenerative cells and plasma rich in growth factors: A first-in-human case report and literature review. *World J Stem Cells* 2019; **11**: 124-146 [PMID: 30842809 DOI: 10.4252/wjsc.v11.i2.124]
24 **Alt EU**, Schmitz C, Bai X. Fundamentals of stem cells: why and how patients' own adult stem cells are the next generation of medicine; 2019. Preprints, 2019040200. Cited February 17, 2019. [DOI: 10.20944/preprints201904.0200.v1]
25 **Hurd J**. Safety and efficacy adipose-derived stem cell injection partial thickness rotator cuff tears. [accessed on May 5th, 2019]. In: ClinicalTrials.gov [Internet]. Available from: https://www.clinicaltrials.gov/ct2/show/NCT02918136 ClinicalTrials.gov Identifier: NCT02918136
26 **Coots BK**. Healing chronic venous stasis wounds with autologous cell therapy. [accessed on May 5th, 2019] In: ClinicalTrials.gov [Internet]. Available from: https://www.clinicaltrials.gov/ct2/show/NCT02961699 ClinicalTrials.gov Identifier: NCT02961699
27 **Boetel T**. Safety of adipose-derived regenerative cells injection for treatment of osteoarthritis of the facet joint. [accessed on May 5th, 2019] In: ClinicalTrials.gov [Internet]. Available from: https://www.clinicaltrials.gov/ct2/show/NCT03513731 ClinicalTrials.gov Identifier: NCT03513731
28 **Hurd J**. Autologous adult adipose-derived regenerative cell injection into chronic partial-thickness rotator cuff tears. [accessed on May 5th, 2019] In: ClinicalTrials.gov [Internet]. Available from: https://www.clinicaltrials.gov/ct2/show/NCT03752827 ClinicalTrials.gov Identifier: NCT03752827
29 **Vandermark R**. Healing osteoarthritic joints in the wrist with adult ADRCs. [accessed on May 5th, 2019] In: ClinicalTrials.gov [Internet]. Available from: https://www.clinicaltrials.gov/ct2/show/NCT03503305 ClinicalTrials.gov Identifier: NCT03503305
30 **Bourin P**, Bunnell BA, Casteilla L, Dominici M, Katz AJ, March KL, Redl H, Rubin JP, Yoshimura K, Gimble JM. Stromal cells from the adipose tissue-derived stromal vascular fraction and culture expanded adipose tissue-derived stromal/stem cells: a joint statement of the International Federation for Adipose Therapeutics and Science (IFATS) and the International Society for Cellular Therapy (ISCT). *Cytotherapy* 2013; **15**: 641-648 [PMID: 23570660 DOI: 10.1016/j.jcyt.2013.02.006]
31 **Bai X**, Yan Y, Coleman M, Wu G, Rabinovich B, Seidensticker M, Alt E. Tracking long-term survival of intramyocardially delivered human adipose tissue-derived stem cells using bioluminescence imaging. *Mol Imaging Biol* 2011; **13**: 633-645 [PMID: 20730500 DOI: 10.1007/s11307-010-0392-z]
32 **Simonetti OP**, Kim RJ, Fieno DS, Hillenbrand HB, Wu E, Bundy JM, Finn JP, Judd RM. An improved MR imaging technique for the visualization of myocardial infarction. *Radiology* 2001; **218**: 215-223 [PMID: 11152805 DOI: 10.1148/radiology.218.1.r01ja50215]
33 **Hunold P**, Vogt FM, Heemann UW, Zimmermann U, Barkhausen J. Myocardial mass and volume measurement of hypertrophic left ventricles by MRI--study in dialysis patients examined before and after dialysis. *J Cardiovasc Magn Reson* 2003; **5**: 553-561 [PMID: 14664133 DOI: 10.1081/JCMR-120025230]
34 **Flett AS**, Hasleton J, Cook C, Hausenloy D, Quarta G, Ariti C, Muthurangu V, Moon JC. Evaluation of techniques for the quantification of myocardial scar of differing etiology using cardiac magnetic resonance. *JACC Cardiovasc Imaging* 2011; **4**: 150-156 [PMID: 21329899 DOI: 10.1016/j.jcmg.2010.11.015]
35 **Cerqueira MD**, Weissman NJ, Dilsizian V, Jacobs AK, Kaul S, Laskey WK, Pennell DJ, Rumberger JA, Ryan T, Verani MS; American Heart Association Writing Group on Myocardial Segmentation and Registration for Cardiac Imaging. Standardized myocardial segmentation and nomenclature for

tomographic imaging of the heart. A statement for healthcare professionals from the Cardiac Imaging Committee of the Council on Clinical Cardiology of the American Heart Association. *Int J Cardiovasc Imaging* 2002; **18**: 539-542 [PMID: 12135124 DOI: 10.1067/mnc.2002.123122]

36 **Ponikowski P**, Voors AA, Anker SD, Bueno H, Cleland JGF, Coats AJS, Falk V, González-Juanatey JR, Harjola VP, Jankowska EA, Jessup M, Linde C, Nihoyannopoulos P, Parissis JT, Pieske B, Riley JP, Rosano GMC, Ruilope LM, Ruschitzka F, Rutten FH, van der Meer P; ESC Scientific Document Group. 2016 ESC Guidelines for the diagnosis and treatment of acute and chronic heart failure: The Task Force for the diagnosis and treatment of acute and chronic heart failure of the European Society of Cardiology (ESC)Developed with the special contribution of the Heart Failure Association (HFA) of the ESC. *Eur Heart J* 2016; **37**: 2129-2200 [PMID: 27206819 DOI: 10.1093/eurheartj/ehw128]

37 **Reiter U**, Reiter G, Manninger M, Adelsmayr G, Schipke J, Alogna A, Rajces A, Stalder AF, Greiser A, Mühlfeld C, Scherr D, Post H, Pieske B, Fuchsjäger M. Early-stage heart failure with preserved ejection fraction in the pig: a cardiovascular magnetic resonance study. *J Cardiovasc Magn Reson* 2016; **18**: 63 [PMID: 27688028 DOI: 10.1186/s12968-016-0283-9].]

38 **Johnston PV**, Sasano T, Mills K, Evers R, Lee ST, Smith RR, Lardo AC, Lai S, Steenbergen C, Gerstenblith G, Lange R, Marbán E. Engraftment, differentiation, and functional benefits of autologous cardiosphere-derived cells in porcine ischemic cardiomyopathy. *Circulation* 2009; **120**: 1075-1083, 7 p following 1083 [PMID: 19738142 DOI: 10.1161/CIRCULATIONAHA.108.816058]

39 **Blázquez R**, Sánchez-Margallo FM, Crisóstomo V, Báez C, Maestre J, Álvarez V, Casado JG. Intrapericardial Delivery of Cardiosphere-Derived Cells: An Immunological Study in a Clinically Relevant Large Animal Model. *PLoS One* 2016; **11**: e0149001 [PMID: 26866919 DOI: 10.1371/journal.pone.0149001]

40 **Tseliou E**, Kanazawa H, Dawkins J, Gallet R, Kreke M, Smith R, Middleton R, Valle J, Marbán L, Kar S, Makkar R, Marbán E. Widespread Myocardial Delivery of Heart-Derived Stem Cells by Nonocclusive Triple-Vessel Intracoronary Infusion in Porcine Ischemic Cardiomyopathy: Superior Attenuation of Adverse Remodeling Documented by Magnetic Resonance Imaging and Histology. *PLoS One* 2016; **11**: e0144523 [PMID: 26784932 DOI: 10.1371/journal.pone.0144523]

41 **Dariolli R**, Naghetini MV, Marques EF, Takimura CK, Jensen LS, Kiers B, Tsutsui JM, Mathias W, Lemos Neto PA, Krieger JE. Allogeneic pASC transplantation in humanized pigs attenuates cardiac remodeling post-myocardial infarction. *PLoS One* 2017; **12**: e0176412 [PMID: 28448588 DOI: 10.1371/journal.pone.0176412]

42 **Natsumeda M**, Florea V, Rieger AC, Tompkins BA, Banerjee MN, Golpanian S, Fritsch J, Landin AM, Kashikar ND, Karantalis V, Loescher VY, Hatzistergos KE, Bagno L, Sanina C, Mushtaq M, Rodriguez J, Rosado M, Wolf A, Collon K, Vincent L, Kanelidis AJ, Schulman IH, Mitrani R, Heldman AW, Balkan W, Hare JM. A Combination of Allogeneic Stem Cells Promotes Cardiac Regeneration. *J Am Coll Cardiol* 2017; **70**: 2504-2515 [PMID: 29145950 DOI: 10.1016/j.jacc.2017.09.036]

43 **Gomez-Mauricio RG**, Acarregui A, Sánchez-Margallo FM, Crisóstomo V, Gallo I, Hernández RM, Pedraz JL, Orive G, Martín-Cancho MF. A preliminary approach to the repair of myocardial infarction using adipose tissue-derived stem cells encapsulated in magnetic resonance-labelled alginate microspheres in a porcine model. *Eur J Pharm Biopharm* 2013; **84**: 29-39 [PMID: 23266493 DOI: 10.1016/j.ejpb.2012.11.028]

44 **Houtgraaf JH**, de Jong R, Kazemi K, de Groot D, van der Spoel TI, Arslan F, Hoefer I, Pasterkamp G, Itescu S, Zijlstra F, Geleijnse ML, Serruys PW, Duckers HJ. Intracoronary infusion of allogeneic mesenchymal precursor cells directly after experimental acute myocardial infarction reduces infarct size, abrogates adverse remodeling, and improves cardiac function. *Circ Res* 2013; **113**: 153-166 [PMID: 23658436 DOI: 10.1161/CIRCRESAHA.112.300730]

45 **Gómez-Mauricio G**, Moscoso I, Martín-Cancho MF, Crisóstomo V, Prat-Vidal C, Báez-Díaz C, Sánchez-Margallo FM, Bernad A. Combined administration of mesenchymal stem cells overexpressing IGF-1 and HGF enhances neovascularization but moderately improves cardiac regeneration in a porcine model. *Stem Cell Res Ther* 2016; **7**: 94 [PMID: 27423905 DOI: 10.1186/s13287-016-0350-z]

46 **Mu D**, Zhang XL, Xie J, Yuan HH, Wang K, Huang W, Li GN, Lu JR, Mao LJ, Wang L, Cheng L, Mai XL, Yang J, Tian CS, Kang LN, Gu R, Zhu B, Xu B. Intracoronary Transplantation of Mesenchymal Stem Cells with Overexpressed Integrin-Linked Kinase Improves Cardiac Function in Porcine Myocardial Infarction. *Sci Rep* 2016; **6**: 19155 [PMID: 26750752 DOI: 10.1038/srep19155]

47 **Hare JM**, DiFede DL, Rieger AC, Florea V, Landin AM, El-Khorazaty J, Khan A, Mushtaq M, Lowery MH, Byrnes JJ, Hendel RC, Cohen MG, Alfonso CE, Valasaki K, Pujol MV, Golpanian S, Ghersin E, Fishman JE, Pattany P, Gomes SA, Delgado C, Miki R, Abuzeid F, Vidro-Casiano M, Premer C, Medina A, Porras V, Hatzistergos KE, Anderson E, Mendizabal A, Mitrani R, Heldman AW. Randomized Comparison of Allogeneic Versus Autologous Mesenchymal Stem Cells for Nonischemic Dilated Cardiomyopathy: POSEIDON-DCM Trial. *J Am Coll Cardiol* 2017; **69**: 526-537 [PMID: 27856208 DOI: 10.1016/j.jacc.2016.11.009]

48 **Kim SW**, Choi JW, Lee CY, Lee J, Shin S, Lim S, Lee S, Kim IK, Lee HB, Hwang KC. Effects of donor age on human adipose-derived adherent stromal cells under oxidative stress conditions. *J Int Med Res* 2018; **46**: 951-964 [PMID: 28984178 DOI: 10.1177/0300060517731684]

49 **Maceira AM**, Prasad SK, Khan M, Pennell DJ. Normalized left ventricular systolic and diastolic function by steady state free precession cardiovascular magnetic resonance. *J Cardiovasc Magn Reson* 2006; **8**: 417-426 [PMID: 16755827 DOI: 10.1080/10976640600572889]

50 **Hare JM**, Fishman JE, Gerstenblith G, DiFede Velazquez DL, Zambrano JP, Suncion VY, Tracy M, Ghersin E, Johnston PV, Brinker JA, Breton E, Davis-Sproul J, Schulman IH, Byrnes J, Mendizabal AM, Lowery MH, Rouy D, Altman P, Wong Po Foo C, Ruiz P, Amador A, Da Silva J, McNiece IK, Heldman AW, George R, Lardo A. Comparison of allogeneic vs autologous bone marrow–derived mesenchymal stem cells delivered by transendocardial injection in patients with ischemic cardiomyopathy: the POSEIDON randomized trial. *JAMA* 2012; **308**: 2369-2379 [PMID: 23117550 DOI: 10.1001/jama.2012.25321]

51 **Kanelidis AJ**, Premer C, Lopez J, Balkan W, Hare JM. Route of Delivery Modulates the Efficacy of Mesenchymal Stem Cell Therapy for Myocardial Infarction: A Meta-Analysis of Preclinical Studies and Clinical Trials. *Circ Res* 2017; **120**: 1139-1150 [PMID: 28031416 DOI: 10.1161/CIRCRESAHA.116.309819]

52 **Suncion VY**, Ghersin E, Fishman JE, Zambrano JP, Karantalis V, Mandel N, Nelson KH, Gerstenblith G, DiFede Velazquez DL, Breton E, Sitammagari K, Schulman IH, Taldone SN, Williams AR, Sanina C, Johnston PV, Brinker J, Altman P, Mushtaq M, Trachtenberg B, Mendizabal AM, Tracy M, Da Silva J,

McNiece IK, Lardo AC, George RT, Hare JM, Heldman AW. Does transendocardial injection of mesenchymal stem cells improve myocardial function locally or globally?: An analysis from the Percutaneous Stem Cell Injection Delivery Effects on Neomyogenesis (POSEIDON) randomized trial. *Circ Res* 2014; **114**: 1292-1301 [PMID: 24449819 DOI: 10.1161/CIRCRESAHA.114.302854]

53 **Hong SJ**, Hou D, Brinton TJ, Johnstone B, Feng D, Rogers P, Fearon WF, Yock P, March KL. Intracoronary and retrograde coronary venous myocardial delivery of adipose-derived stem cells in swine infarction lead to transient myocardial trapping with predominant pulmonary redistribution. *Catheter Cardiovasc Interv* 2014; **83**: E17-E25 [PMID: 22972685 DOI: 10.1002/ccd.24659]

54 **Oberbauer E**, Steffenhagen C, Wurzer C, Gabriel C, Redl H, Wolbank S. Enzymatic and non-enzymatic isolation systems for adipose tissue-derived cells: current state of the art. *Cell Regen (Lond)* 2015; **4**: 7 [PMID: 26435835 DOI: 10.1186/s13619-015-0020-0]

55 **van Dongen JA**, Tuin AJ, Spiekman M, Jansma J, van der Lei B, Harmsen MC. Comparison of intraoperative procedures for isolation of clinical grade stromal vascular fraction for regenerative purposes: a systematic review. *J Tissue Eng Regen Med* 2018; **12**: e261-e274 [PMID: 28084666 DOI: 10.1002/term.2407]

56 **Shah FS**, Wu X, Dietrich M, Rood J, Gimble JM. A non-enzymatic method for isolating human adipose tissue-derived stromal stem cells. *Cytotherapy* 2013; **15**: 979-985 [PMID: 23725689 DOI: 10.1016/j.jcyt.2013.04.001]

57 **Røsland GV**, Svendsen A, Torsvik A, Sobala E, McCormack E, Immervoll H, Mysliwietz J, Tonn JC, Goldbrunner R, Lønning PE, Bjerkvig R, Schichor C. Long-term cultures of bone marrow-derived human mesenchymal stem cells frequently undergo spontaneous malignant transformation. *Cancer Res* 2009; **69**: 5331-5339 [PMID: 19509230 DOI: 10.1158/0008-5472.CAN-08-4630]

58 **Xu S**, De Becker A, De Raeve H, Van Camp B, Vanderkerken K, Van Riet I. In vitro expanded bone marrow-derived murine (C57Bl/KaLwRij) mesenchymal stem cells can acquire CD34 expression and induce sarcoma formation in vivo. *Biochem Biophys Res Commun* 2012; **424**: 391-397 [PMID: 22771324 DOI: 10.1016/j.bbrc.2012.06.118]

59 **Pan Q**, Fouraschen SM, de Ruiter PE, Dinjens WN, Kwekkeboom J, Tilanus HW, van der Laan LJ. Detection of spontaneous tumorigenic transformation during culture expansion of human mesenchymal stromal cells. *Exp Biol Med (Maywood)* 2014; **239**: 105-115 [PMID: 24227633 DOI: 10.1177/1535370213506802]

60 **Badimon L**, Oñate B, Vilahur G. Adipose-derived Mesenchymal Stem Cells and Their Reparative Potential in Ischemic Heart Disease. *Rev Esp Cardiol (Engl Ed)* 2015; **68**: 599-611 [PMID: 26028258 DOI: 10.1016/j.rec.2015.02.025]

61 **Mitchell JB**, McIntosh K, Zvonic S, Garrett S, Floyd ZE, Kloster A, Di Halvorsen Y, Storms RW, Goh B, Kilroy G, Wu X, Gimble JM. Immunophenotype of human adipose-derived cells: temporal changes in stromal-associated and stem cell-associated markers. *Stem Cells* 2006; **24**: 376-385 [PMID: 16322640 DOI: 10.1634/stemcells.2005-0234]

62 **Maumus M**, Peyrafitte JA, D'Angelo R, Fournier-Wirth C, Bouloumié A, Casteilla L, Sengenès C, Bourin P. Native human adipose stromal cells: localization, morphology and phenotype. *Int J Obes (Lond)* 2011; **35**: 1141-1153 [PMID: 21266947 DOI: 10.1038/ijo.2010.269]

63 **Yoshimura K**, Shigeura T, Matsumoto D, Sato T, Takaki Y, Aiba-Kojima E, Sato K, Inoue K, Nagase T, Koshima I, Gonda K. Characterization of freshly isolated and cultured cells derived from the fatty and fluid portions of liposuction aspirates. *J Cell Physiol* 2006; **208**: 64-76 [PMID: 16557516 DOI: 10.1002/jcp.20636]

64 **Alt E**, Yan Y, Gehmert S, Song YH, Altman A, Gehmert S, Vykoukal D, Bai X. Fibroblasts share mesenchymal phenotypes with stem cells, but lack their differentiation and colony-forming potential. *Biol Cell* 2011; **103**: 197-208 [PMID: 21332447 DOI: 10.1042/BC20100117]

65 **Ozerdem U**, Grako KA, Dahlin-Huppe K, Monosov E, Stallcup WB. NG2 proteoglycan is expressed exclusively by mural cells during vascular morphogenesis. *Dev Dyn* 2001; **222**: 218-227 [PMID: 11668599 DOI: 10.1002/dvdy.1200]

66 **Suzuki S**, Namiki J, Shibata S, Mastuzaki Y, Okano H. The neural stem/progenitor cell marker nestin is expressed in proliferative endothelial cells, but not in mature vasculature. *J Histochem Cytochem* 2010; **58**: 721-730 [PMID: 20421592 DOI: 10.1369/jhc.2010.955609]

67 **Masson K**, Rönnstrand L. Oncogenic signaling from the hematopoietic growth factor receptors c-Kit and Flt3. *Cell Signal* 2009; **21**: 1717-1726 [PMID: 19540337 DOI: 10.1016/j.cellsig.2009.06.002]

68 **Dominici M**, Le Blanc K, Mueller I, Slaper-Cortenbach I, Marini F, Krause D, Deans R, Keating A, Prockop Dj, Horwitz E. Minimal criteria for defining multipotent mesenchymal stromal cells. The International Society for Cellular Therapy position statement. *Cytotherapy* 2006; **8**: 315-317 [PMID: 16923606 DOI: 10.1080/14653240600855905]

69 **Bai X**, Yan Y, Song YH, Seidensticker M, Rabinovich B, Metzele R, Bankson JA, Vykoukal D, Alt E. Both cultured and freshly isolated adipose tissue-derived stem cells enhance cardiac function after acute myocardial infarction. *Eur Heart J* 2010; **31**: 489-501 [PMID: 20037143 DOI: 10.1093/eurheartj/ehp568]

70 **Fotuhi P**, Song YH, Alt E. Electrophysiological consequence of adipose-derived stem cell transplantation in infarcted porcine myocardium. *Europace* 2007; **9**: 1218-1221 [PMID: 17951268 DOI: 10.1093/europace/eum224]

71 **Anderson LJ**, Holden S, Davis B, Prescott E, Charrier CC, Bunce NH, Firmin DN, Wonke B, Porter J, Walker JM, Pennell DJ. Cardiovascular T2-star (T2*) magnetic resonance for the early diagnosis of myocardial iron overload. *Eur Heart J* 2001; **22**: 2171-2179 [PMID: 11913479 DOI: 10.1053/euhj.2001.2822]

72 **Yang D**, Wang W, Li L, Peng Y, Chen P, Huang H, Guo Y, Xia X, Wang Y, Wang H, Wang WE, Zeng C. The relative contribution of paracine effect versus direct differentiation on adipose-derived stem cell transplantation mediated cardiac repair. *PLoS One* 2013; **8**: e59020 [PMID: 23527076 DOI: 10.1371/journal.pone.0059020]

73 **Liu Z**, Xu Y, Wan Y, Gao J, Chu Y, Li J. Exosomes from adipose-derived mesenchymal stem cells prevent cardiomyocyte apoptosis induced by oxidative stress. *Cell Death Discov* 2019; **5**: 79 [PMID: 30911413 DOI: 10.1038/s41420-019-0159-5]

74 **Vujic A**, Lerchenmüller C, Wu TD, Guillermier C, Rabolli CP, Gonzalez E, Senyo SE, Liu X, Guerquin-Kern JL, Steinhauser ML, Lee RT, Rosenzweig A. Exercise induces new cardiomyocyte generation in the adult mammalian heart. *Nat Commun* 2018; **9**: 1659 [PMID: 29695718 DOI: 10.1038/s41467-018-04083-1]

75 **Gnecchi M**, Zhang Z, Ni A, Dzau VJ. Paracrine mechanisms in adult stem cell signaling and therapy. *Circ*

Res 2008; **103**: 1204-1219 [PMID: 19028920 DOI: 10.1161/CIRCRESAHA.108.176826]
76 **Rota M**, Padin-Iruegas ME, Misao Y, De Angelis A, Maestroni S, Ferreira-Martins J, Fiumana E, Rastaldo R, Arcarese ML, Mitchell TS, Boni A, Bolli R, Urbanek K, Hosoda T, Anversa P, Leri A, Kajstura J. Local activation or implantation of cardiac progenitor cells rescues scarred infarcted myocardium improving cardiac function. *Circ Res* 2008; **103**: 107-116 [PMID: 18556576 DOI: 10.1161/CIRCRESAHA.108.178525]
77 **Sanganalmath SK**, Bolli R. Cell therapy for heart failure: a comprehensive overview of experimental and clinical studies, current challenges, and future directions. *Circ Res* 2013; **113**: 810-834 [PMID: 23989721 DOI: 10.1161/CIRCRESAHA.113.300219]
78 **Ohnishi S**, Sumiyoshi H, Kitamura S, Nagaya N. Mesenchymal stem cells attenuate cardiac fibroblast proliferation and collagen synthesis through paracrine actions. *FEBS Lett* 2007; **581**: 3961-3966 [PMID: 17662720 DOI: 10.1016/j.febslet.2007.07.028]
79 **Schmitz C**, Hof PR. Design-based stereology in neuroscience. *Neuroscience* 2005; **130**: 813-831 [PMID: 15652981 DOI: 10.1016/j.neuroscience.2004.08.050]
80 **Bergmann O**, Zdunek S, Felker A, Salehpour M, Alkass K, Bernard S, Sjostrom SL, Szewczykowska M, Jackowska T, Dos Remedios C, Malm T, Andrä M, Jashari R, Nyengaard JR, Possnert G, Jovinge S, Druid H, Frisén J. Dynamics of Cell Generation and Turnover in the Human Heart. *Cell* 2015; **161**: 1566-1575 [PMID: 26073943 DOI: 10.1016/j.cell.2015.05.026]

Published By Baishideng Publishing Group Inc
7041 Koll Center Parkway, Suite 160, Pleasanton, CA 94566, USA
Telephone: +1-925-2238242
E-mail: bpgoffice@wjgnet.com
Help Desk: https://www.f6publishing.com/helpdesk
https://www.wjgnet.com